Journal of Geochemical Exploration 160 (2016) 16–30

Contents lists available at ScienceDirect

Journal of Geochemical Exploration

journal homepage: www.elsevier.com/locate/jgeoexp

Gold and silver in a system of sulfide tailings. Part 1: Migration in water flow

I.N. Myagkaya [a,*], E.V. Lazareva [a], M.A. Gustaytis [a,b], S.M. Zhmodik [a,b]

[a] V.S. Sobolev Institute of Geology and Mineralogy, Siberian Branch of Russian Academy of Sciences, 3, Koptyug Ave. Novosibirsk 630090, Russia
[b] Novosibirsk State University, 3, Pirogov Str. Novosibirsk 630090, Russia

ARTICLE INFO

Article history:
Received 30 April 2015
Revised 2 September 2015
Accepted 3 October 2015
Available online 9 October 2015

Keywords:
Gold cyanidation
Sulfide wastes
Acid mine drainage
Surface and pore waters
Migration
Speciation
Gold
Silver

ABSTRACT

Wastes of the ore cyanide process are prone to oxidation and acid leaching that cause mobilization, migration, and precipitation of elements, including noble metals. The issues of waste oxidation, as well as release and transport of oxidation products, are of principal environmental concern and a focus of active geochemical research. We study the behavior of Au and Ag in the natural–industrial system "sulfide wastes–surface/pore waters–particulate matter–bottom sediments" in the presence of different elements (Na, Mg, K, Ca, Al, Fe, Cu, Zn, Se, Ag, Au, Hg, Pb, REE, etc.), at the Novo-Ursk auriferous pyritic deposit (Salair, Kemerovo region, Russia).

The wastes include processed primary ore (wastes I) and ore from the gold-bearing weathering profile (wastes II) that store, respectively, 0.5 ppm Au, 18 ppm Ag and 0.26 ppm Au, 13 ppm Ag. Gold in wastes I occurs in the native form with Cu and Ag impurities and also Au exist as invisible species in pyrite. In wastes II, gold is adsorbed onto the surfaces of secondary mineral particles (kaolinite, montmorillonite, hydromica, and Fe(III) compounds) while silver is an isomorphic impurity in alunite–jarosite minerals. The oxidation of wastes produces acid mine drainage (AMD) water, with pH = 1.9 and high concentrations of sulfate, Fe, Al, Cu, Zn, Pb, As, Se, Te, Hg, Cd, and REE, which flows into the Ur River (a tributary of the Inya).

The stream transports gold and silver existing in dissolved + colloidal and particulate forms. Dissolved + colloidal gold and silver have similar distribution patterns with their contents inversely proportional to pH. Dissolved + colloidal gold in the AMD water is more abundant than silver (0.4–1.2 ppb Au against 0.1–0.3 ppb Ag). Gold changes from the dissolved + colloidal (in AMD) to particulate (till 0.03 ppb) forms and precipitates in progressively larger amounts with distance from the tailings. Silver in most of the analyzed natural and tailings-impacted waters exists as suspended particles (to 1 ppb). The concentrations of gold and silver are the highest (1.8–2.1 ppb Au and 4.5–5.7 ppb Ag) in peat pore waters within the geochemical trains of the tailings, apparently as a result of re-precipitation on organic barriers.

1. Introduction

Wastes of mining and ore processing have been studied for years in various aspects. The available knowledge on the structure of tailings, as well as on mineralogy, geochemistry, and microbiology of weathering profiles are synthesized in numerous publications (Alpers et al., 1994; Blowes et al., 1994, 2003; Jambor, 1994; Ritchie, 1994; Bigham et al., 1996; Nordstrom, 2000; Dold and Fontbote, 2002; Lazareva et al., 2002; Descostes et al., 2004; Druschel et al., 2004; Gleisner et al., 2006; Equeenuddin et al., 2010; Marescotti et al., 2012; Auld et al., 2013; Sun et al., 2013). This knowledge is especially important as having implications for prevention, treatment, and remediation of contamination effects (Gitari et al., 2008; Ríos et al., 2008; Nyquis and Greger, 2009; Dold et al., 2009; Gibert et al., 2011; Macías et al., 2012; Heviánková et al., 2014; Jeen et al., 2014).

Sulfide wastes deposited in open air are exposed to wind and water weathering and related oxidation, which contaminates large areas around producing geochemical dispersion haloes and trains (de Haan, 1991; Bortnikova et al., 2003; Moncur et al., 2014). Acid sulfate mine drainage waters formed by oxidation of sulfide materials bear high concentrations of dissolved solids, including heavy metals and toxic elements (Bigham, 1994; Nordstrom and Alpers, 1999; Plumlee, 1999; Seal and Hammarstrom, 2003; Blowes et al., 2003; Valente and Gomes, 2009; Luptakova et al., 2012). Acid mine drainage (AMD) contains abundant sulfate anions and other sulfur ions, such as tetrathionate ($S_4O_6^{2-}$; reaction 1) (Mironov et al., 1989) and thiosulfate ($S_2O_3^{2-}$; reaction 2), according to Pourbaix diagrams (Xia, 2008). Thiosulfate is metastable in the oxide zone and transforms either into tetrathionate ($S_4O_6^{2-}$) or trithionate ($S_3O_6^{2-}$) depending on pH (reactions 3–5); the two latter ions, in turn, become oxidized to SO_3^{2-}, $S_2O_6^{2-}$ and SO_4^{2-} (Xia, 2008).

$$4FeS_2 + 11O_2 + 4H_2O = 2FeSO_4 + 2Fe(OHSO_4) + H_2S_4O_6 + H_2O \quad (1)$$

$$2S^{2-} + 4S_4O_6^{2-} + 6OH^- = 9S_2O_3^{2-} + 3H_2O \quad (2)$$

* Corresponding author.
E-mail address: i_myagkaya@igm.nsc.ru (I.N. Myagkaya).

http://dx.doi.org/10.1016/j.gexplo.2015.10.004
0375-6742/

$$3S_2O_3^{2-} + 2O_2 + H_2O = 2S_3O_6^{2-} + 2OH^- \quad (3)$$

$$4S_2O_3^{2-} + O_2 + 2H_2O = 2S_4O_6^{2-} + 4OH^- \quad (4)$$

$$3S_4O_6^{2-} + 2.5O_2 + 2OH^- = 4S_3O_6^{2-} + H_2O. \quad (5)$$

Elements released from AMD waters become redeposited as ochreous precipitates. Goethite, ferrihydrite, lepidocrocite, jarosite, schwertmannite, and hydrogoethite are main ochreous minerals (Bigham, 1994; Bigham et al., 1996; Marescotti et al., 2012). Iron hydroxides, with their high sorption capacity, commonly adsorb heavy metals and other AMD elements, but ochreous precipitates are unstable and prone to redissolution by acid waters with pH 4.5–6.5 (McDonald et al., 2006; Herrera et al., 2007), which poses pollution problems (Jarvis and Rees, 2004; Carbone et al., 2013). Minor pH–Eh changes can trigger rapid mineral evolution including dissolution, re-precipitation, and structure changes (Marescotti et al., 2012), which return heavy metals back to the waters and maintain widespread of low-density fine-grained ochreous precipitates (Hammarstrom et al., 2003).

The environmental issues concerning acid mine drainage and ochreous precipitates (Hammarstrom et al., 2005; Valente and Gomes, 2009; Sima et al., 2011; Luptakova et al., 2012), and the related contamination (Sarmiento et al., 2011; Carbone et al., 2013), arouse special interest. Most of the research in this line has reasonably focused on the behavior of heavy metals and toxic elements (As, Hg, etc.) (Boulet and Larocque, 1998; Jung, 2001; Lazareva et al., 2002; Al et al., 2006; Roychoudhury and Starke, 2006; Gustaytis et al., 2010, 2013; Equeenuddin et al., 2013; Lusilao-Makiese et al., 2013; Rieuwerts et al., 2014), while noble metals (Au and Ag) in tailings remain little explored (Stoffregen, 1986; Mironov et al., 1989; Benedetti and Boulegue, 1991; Leybourne et al., 2000; Dutova et al., 2006; Reith and McPhail, 2007; Myagkaya et al., 2013).

The behavior of gold in the superficial conditions of oxidation and weathering in gold fields and their surroundings has been mostly studied in terms of distribution patterns, speciation, and morphology of particles (Roslyakov, 1981; Vasconcelos and Kyle, 1991; Lawrance and Griffin, 1994; Bortnikova et al., 1996; de Oliveira and de Oliveira, 2000; Kalinin et al., 2009; Hough et al., 2011; Zhmodik et al., 2012; Reith et al., 2012; Fairbrother et al., 2012). However, some recent papers consider migration paths of gold in mining and refinery wastes (Benedetti and Boulegue, 1991; Leybourne et al., 2000; Al et al., 2006; Roychoudhury and Starke, 2006) and postulate its high mobility in natural and manmade supergene environments (Mann, 1984; Vlassopoulos and Wood, 1990; Vlassopoulos et al., 1990; Andrade et al., 1991; Benedetti and Boulegue, 1991; Bowell, 1992; Cidu et al., 1995; Radomskaya et al., 2005; Dutova et al., 2006). Additionally, geochemical cycling of Au in supergene environments can be mediated by microorganisms (Korobushkina and Korobushkin, 1998; Reith et al., 2005, 2012; Reith and McPhail, 2007; Southam and Beveridge, 1994; Southam et al., 2009).

Gold migrating in streams is most often dissolved or particulate. Dissolved gold is present in both natural and mine waters as part of chlorine-, sulfur-, or hydro-complexes, cyanide, as well as mixed Au complexes (Stoffregen, 1986; Vlassopoulos and Wood, 1990; Andrade et al., 1991; Benedetti and Boulegue, 1991; Tossell, 1996; Leybourne et al., 2000; Radomskaya et al., 2005; Dutova et al., 2006; Xia, 2008). As Pourbaix diagrams show, $AuOH(H_2O)^0$ (Vlassopoulos and Wood, 1990), and mixed Cl and S complexes such as AuH_2S^+ and $AuOHCl^-$ (Dutova et al., 2006), control gold solubility in most of natural waters (pH to ~6–12). Given the presence of Cl^-, the chloride ($AuCl_2^-$, $AuCl_4^-$, $AuOHCl^-$) and sulfide ($Au(S_2O_3)_2^{3-}$ and $Au(HS)_2^-$) complexes are the major agents in acid sulfate waters (Mann, 1984; Stoffregen, 1986; Vlassopoulos and Wood, 1990; Andrade et al., 1991; Colin and Vieillard, 1991; Dutova et al., 2006). Thiosulfate Au complexes in acid waters exist according to reaction 6 (Xia, 2008). Furthermore, drainage solutions may contain cyanide complexes $Au(CN)_2^-$ that result from oxidative dissolution of wastes (Leybourne et al., 2000).

$$4Au^0 + 8S_2O_3^{2-} + O_2 + 2H_2O = 4Au(S_2O_3)_2^{3-} + 4OH^- \quad (6)$$

Particulate gold can form by adsorption onto mineral particles as a result of interaction between hydroxyl groups of colloids and/or cation exchange reactions related to electrostatic interactions. These bonds are relatively weak and the elements are easily desorbed back into water (Sarkar et al., 1999). Second, abundant particulate gold may be due to highly adsorptive amorphous iron hydroxides. Transport of such gold is called mechanic migration (Radomskaya et al., 2005).

Metastable thiosulphate complexes at pH < 5 break down to sulfate, the reaction being catalyzed by transitional elements and bacteria, while gold re-precipitates on iron hydroxide particles (Mironov et al., 1989; Benedetti and Boulegue, 1991; Ran et al., 2002; Yudovich and Ketris, 2004), by reaction 7 (Xia, 2008):

$$Fe^{2+} + Au(S_2O_3)_2^{3-} + 3OH^- = Au^0 + FeOOH + H_2O + 2S_2O_3^{2-} \quad (7)$$

Third, formation of stable colloid particles that can penetrate through a 0.45 μm membrane filter provide the presence of colloids and related elements in filtered water (Petrukhin, 1992; Howe and Clark, 2002; Wang et al., 2003). Fourth, gold can form soluble and insoluble organic complexes which influence its mobility in supergene environments (Baker, 1978; Vlassopoulos et al., 1990; Baranova et al., 1991; Bowell et al., 1993a,b; Varshal et al., 1996, 2000; Wood, 1996). For instance, the carboxyl and phenol groups of humic acids (HA) form strong complexes with noble metals, which affects the HA sorption capacity (Varshal et al., 2000) and acts as a barrier for noble metal ions. Interaction with fulvic acids (FA) also leads to the formation of soluble complexes and increases the mobility of noble metals (Baranova et al., 1991; Bowell et al., 1993a,b). Furthermore, organic acids can reduce ion complexes and provide gold fixation: e.g., humic substances in river water reduce gold from chloride complexes to gold-bearing organic complexes (Baker, 1978). The standard reduction potentials for FA and HA range from +0.5 to +0.7 V, while the species such as $AuCl_4^-$ and $AuC1_2^-$ are abundant only in highly and moderately oxidizing media, respectively; therefore, humic and fulvic acids do not form dissolved complexes with Au(III) and Au(I) (Wood, 1996). In this case, chloride-complexed gold ($AuCl_4^-$, $AuC1_2^-$) becomes reduced and immobilized upon entering the environments where the humic substances have "hard" O-donor groups dominating their binding sites and control the redox conditions. On the other hand, HA cause less influence on reduction and fixation of gold if the Au transporting complexes have low standard reduction potentials (e.g., $AuOH^0$ ($E° = 0.506$ V), $Au(HS)_2^-$ and $Au(S_2O_3)_2^{3-}$), with a relatively high proportion of "soft" N- or S-donor binding sites, whereby strong complexing may lower the standard reduction potentials to prevent reduction and promote aqueous transport (Wood, 1996). Organic substances can also maintain reduction of Au (III) to elemental gold and formation of colloids (Ong and Swanson, 1969; Avramenko et al., 2012).

Our previous studies (Myagkaya et al., 2013) showed that oxidative leaching of wastes in the Ursk tailings led to gold and silver dissolution and re-precipitation on a bio-geochemical barrier of peat lying beneath wastes shed from the stockpiles. That inference has guided the research reported in this publication, which consists of two parts. Part 1 deals with Au and Ag migrations in water, in the presence of different elements (Na, Mg, K, Ca, Al, Fe, Cu, Zn, Se, Ag, Au, Hg, Pb, REE etc.) in natural and mine waters in the system "sulfide wastes–surface/pore waters–particulate matter–bottom sediments" in the Ursk area.

2. Study area

The Ursk tailings site is located at 54°27′11.03″ N, 85°24′09.76″ E in Ursk Village (Kemerovo region, Russia, Fig. 1) within the Ur ore field in

the northern Salair Ridge (Altai-Sayan mountains, Siberia). The tailings have been mined for more than 80 years ago and store wastes from cyaniding auriferous pyritic and complex ores (primary ore and ore from the gold-bearing weathering profile) of the Novo-Ursk deposit (Shcherbakova et al., 2010; Gustaytis et al., 2010, 2013; Myagkaya et al., 2013).

The ore mineralogy consists of pyrite, sphalerite, chalcopyrite, galena, arsenical pyrite, fahlite, cinnabar, as well as quartz, barite, calcite, chlorite-group minerals, sericite, albite, graphite, rutile, and fluorite, with Au and Ag ranges 0.7–4 ppm and 16.5–29.65 ppm, respectively (Bessonenko et al., 1970; Roslyakov et al., 1995; Tokarev et al., 2004).

3. Materials and methods

3.1. Sampling

In the course of field trips in 2011 through 2013, we sampled waters, suspended particles, and bottom sediments within the contamination area around the tailings (Fig. 2). The waters were of three groups: acid mine drainage (AMD) (i) and natural waters in the Ur river, lakes, and ponds sampled upstream (ii) and downstream (iii) of the AMD discharge (W-1 and in W-13–W-16, respectively, in Fig. 2). The AMD waters were sampled at different distances from the tailings (W-4–W-12, Fig. 2) and in different seasons to monitor seasonal changes in water chemistry.

Potentiometry for pH and Eh of all non-acidified and non-filtered sampled waters was performed in situ using a portable Infraspak-Analit Anion 7051 water analyzer (Russia), with an electrode calibrated against standard buffer solutions of pH = 1.68–4.01–6.86–9.18. The absolute errors did not exceed ±0.02 for pH and ±2 for Eh. Dissolved oxygen was measured in situ by titration using a Merck mobile testing set (Germany).

Elements in water can exist in truly dissolved (filter pore size < 0.2 μm), dissolved plus colloidal (filter pore size from 0.2 to < 0.45 μm) and particulate (filter pore size > 0.45 μm) forms (Petrukhin, 1992; Howe and Clark, 2002; Wang et al., 2003). To study Au and Ag partitioning between the dissolved + colloidal and particulate (suspended) fractions, all surface water samples were filtered through 0.45 μm low adsorption cellulose acetate membrane filters (type 11106–47-N) for aqueous solutions (Sartorius Stedim, Germany). The filters combine high flow rates and thermal stability with very low adsorption characteristics, and are therefore perfectly suited for use in pressure filtration devices. The filters were weighed before and after filtering on first-class precise analytic balance (LB 210-A SartoGosm, Russia). The Au and Ag contents in surface waters were estimated with reference to the dissolved + colloidal/particulate species ratio, while those in particulate matter were calculated taking into account the volume of filtered solution, the filter weight, and the amount of filtered material, for further conversion of Au and Ag in the particulate aliquots into their contents in particles suspended in a liter of solution.

Then the filtered water was poured into vials and acidified. All water samples for Hg were poured into Pyrex vials, as borosilicate glass is the best suitable material which can prevent samples from contamination with atmospheric Hg vapor (Hamlin, 1989). We used available conical Falcon (Axygen) polypropylene vials, with low sorption capacity, proceeding from data on adsorption of elements (Cu, Zn, Se, Pb, Na, Mg, Al, Si, K, Ca, Fe, Co, REE, etc.) on the walls of containers made from different materials (polypropylene, borosilicate glass, teflon, etc.) (Robertson, 1968), as well as from the fact that Au can adsorb on both silica (borosilicate) glass (Beneš, 1964; Samiullah, 1985) and polypropylene (Beneš and Smetana, 1966). Samples can be stored from 24 h (Cidu

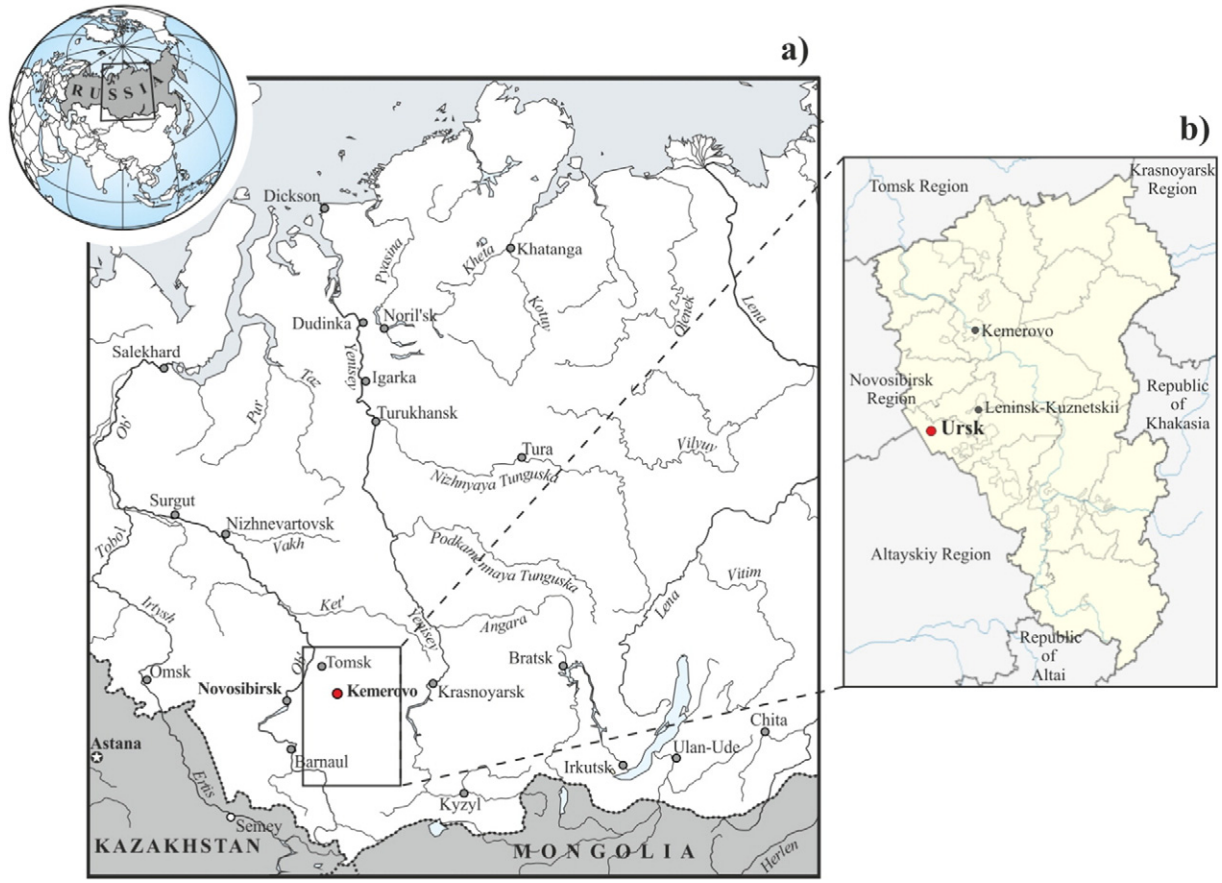

Fig. 1. Location map of Ursk gold mine area (a: map is based on UN map N 3840 Rev. I Nov. 2002; b: map is scaled-up section).

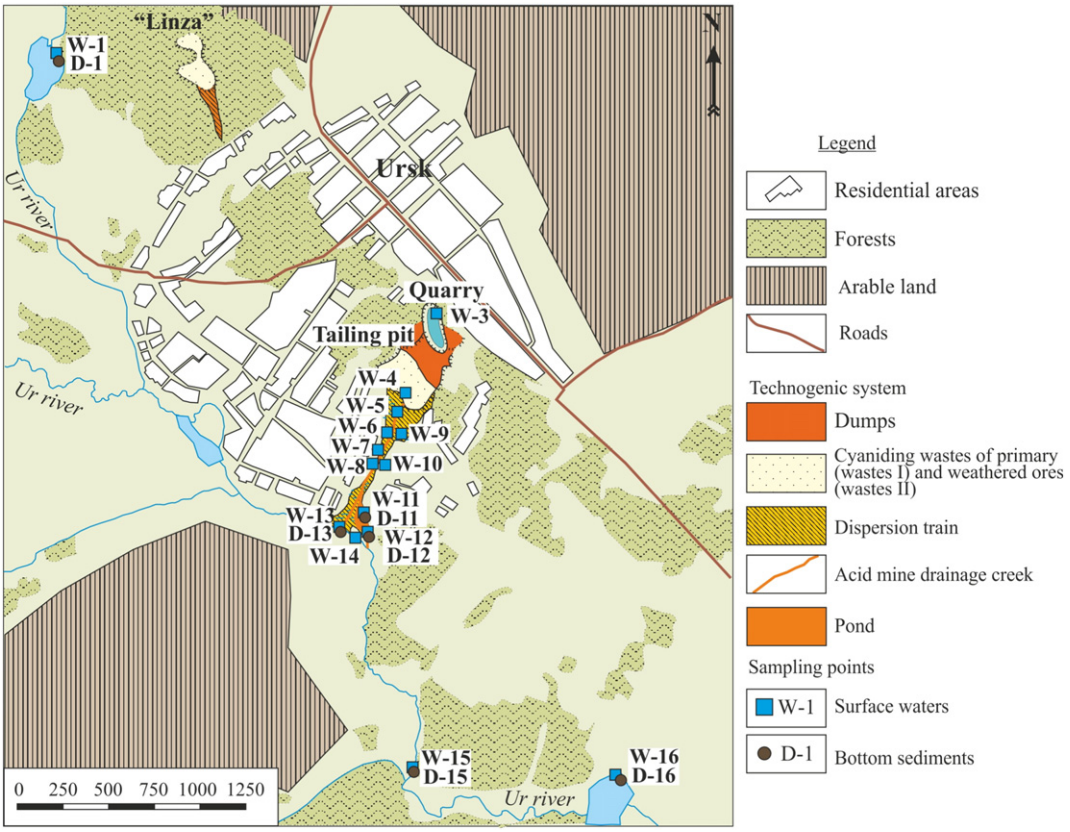

Fig. 2. Sketch map of sampling sites for waters and bottom sediments at the Ursk tailings site located at 54°27′11.03″ N, 85°24′09.76″ E in Ursk Village. Samples (W) represent waters upstream of AMD discharge (W-1), flooded quarry (W-3), AMD under wastes in proximal zone of contamination train (W-4), AMD waters at different distances from the tailings (W-5 to W-10), pond (W-11), pool of AMD flowing from the pond, before discharge into the Ur (W-12), AMD mixed with Ur River (W-13), Ur River, 200 m downstream of AMD discharge (W-14), Ur River, 1–3 km downstream of AMD discharge (W-15 to W-16).

et al., 1994) to one year (Falkner and Edmond, 1990) in polypropylene vials without adsorption losses of Au (the element of our interest) when acidified by aqua regia to pH 1–2. According to the Interstate standardization for water sampling (All-Union State Standard # 31861–2012, 2013), most of analytes are preserved in the solution at pH < 2, the minimum ratio for acidifying being 2:500 for all samples (All-Union State Standard # 31861–2012, 2013). The acidified waters were analyzed immediately upon return from the field. Note that the issues of sorption on container walls and preservation of ultra-trace Au and Ag are of minor importance for this study as they do not interfere much with the general behavior patterns of the elements in the system "natural waters — AMD–AMD-contaminated waters". Some water samples were left non-acidified for determination of major ions. The waters were sampled at 17 points; simultaneously with water sampling, bottom sediment samples were collected into 1 L plastic bottles and packed tightly.

Solids sampled in the contamination train included wastes of primary pyrite ore and those of the gold-bearing weathering profile (wastes of types I and II, respectively), as well as peat in a swampy ravine downstream of the tailings. The wastes of both types and peat were pressed with a portable manual press at 150 g/cm^3 to extract pore water for analysis. Pore waters were sampled and acidified without filtering, as in the case of surface water sampling. Additionally, heavy mineral concentrate (HMC) samples were washed out from peat in the field.

3.2. Experimental procedures

3.2.1. Mineralogy

Solid materials (bottom sediments, peat, wastes, and filter precipitates) were air dried before analysis. Gray HMC samples were washed to black in the field; HMC samples from cyanide wastes were washed additionally on the concentrator. Pyrite monofractions were isolated from washed HMC samples by flotation and electrostatic methods for further Au and Ag determination.

Scanning electron microscopy (SEM) was applied to polished sections and pellets of primary samples of wastes, HMC, pyrite monofractions and peat to study the morphology and identify separate particles. The instruments were a Carl Zeiss LEO1430VP (Germany) and a TESCAN MIRA3 LMU (Czech Republic) scanning electron microscopes with Oxford INCA Energy EDS detectors (UK). The Oxford Instruments INCA Energy 350 spectrometer in the LEO1430VP microscope is designed for micron-scale studies and can record X-ray spectra of elements from B to U, to an optical resolution of 4–4.5 nm. The other microanalyzer INCA Energy 450+ is based on the Oxford Instruments NanoAnalysis X-MAX 80 system and has an optical resolution of 1 nm. The operation conditions were: 15 mm working distance, 20 keV acceleration voltage, and 1.5 nA beam current. The contents of elements in mineral grains smaller than the beam spot (many particles are <1 μm while aggregates are porous) were estimated from relative contents of major elements subtracting the elements of the host mineral. Minerals in wastes and sediments were studied by powder X-ray diffraction (XRD) on a DRON-4 diffractometer operated at 40 kV and 24 mA, with CuK-α radiation.

3.2.2. Major- and trace-element chemistry of wastes, bottom sediments and suspended particles

The contents of major elements in the wastes and bottom sediments were determined by X-ray fluorescence spectroscopy (XRF) in pellets made in the following way. The samples were dried at 105 °C for 1 h, then ignited at 1000 °C for 2.5 h, and then mixed with a flux consisting of 66.67% lithium tetraborate, 32.83% lithium metaborate, and 0.5%

lithium bromide, at 1:9 (total weight of the mixture was 5 g). The mixture was fused in Pt crucibles, in a Linn High Therm Gmbh Lifumat-2.0-Ox induction furnace. The analysis was performed on an ARL-9900-XP X-ray spectrometer (Applied Research Laboratories, Switzerland).

The abundances of C, H, N and S in the same materials of wastes and bottom sediments were determined by the CHNS elemental analysis on an EvroVector Euro EA 3000 analyzer (Italy), using the combustion/gas chromatography techniques. The analysis was by catalytic combustion followed by packed column gas chromatographic separation with thermal conductivity detection (using a single TCD). The analytical accuracy was 0.3–0.5 wt.%, at the range of measured concentrations from 1.5 to 95%.

The contents of Cu, Zn, Se, Rb, Sr, Mo, Cd, Sn, Sb, Te, Hg, As, and Pb in the wastes were determined by X-ray fluorescence spectroscopy with synchrotron radiation (SR-XRF), on a VEPP-3 spectrometer operated at 15 to 50 keV, following the MVI-3-2006 procedure (Daryin, 2006). Samples were prepared as 30 mg compressed pellets, 5–6 mm in diameter, and analyzed to an accuracy of ±30% relative to the absolute abundance. The detection limits for the analyzed elements were 0.0001–0.1 wt.%.

The contents of Cu, Zn, Cd, Pb in the bottom sediments were determined by the atomic absorption spectroscopy (AAS). The AAS analysis was performed using a Thermo Electron Corporation Solar M6 spectrometer with a Zeeman and deuterium background correction system (USA), to an accuracy of 10–35 relative %, at p = 0.95 confidence probability. The detection limits were from 0.05 to $5 \cdot 10^3$ ppm for Cu, Zn, Cd and from 0.5 to $5 \cdot 10^3$ ppm for Pb (M-MVI-80-2008, 2008).

The contents of Au and Ag in solid samples (wastes, bottom sediments and suspended particles) were determined at a certified laboratory of the Institute of Geology and Mineralogy (Novosibirsk) following the procedures from (MVI NSAM N 237-S, 2006; MVI NSAM N 130-S, 2006) modified after the method by Tsimbalist (1984) which was specially designed for evaluation of ultra-trace Ag and Au contents ($n \cdot 10^{-6}$–$n \cdot 10^{-8}$%). The method implies extraction pre-concentration of elements into the organic phase followed by AAS of elements in the extract. Subsample solids (1 g) and weighed membrane filters were acid digested. For silver analysis, samples were digested in aqua regia and HCl, and the solution with silver was sprayed (atomized) in flame to assess the absorption of radiation by free silver atoms. Silver present in contents below 10 ppm was extracted by isopropylamine before flame atomization (MVI NSAM N 130-S, 2006). The samples analyzed for gold were likewise digested in aqua regia and HCl but after being annealed in a muffle furnace at 650 °C (MVI NSAM N 237-S, 2006). The element that was transferred to the acid solution was extracted by toluene solutions of organic sulfides. The extracts were analyzed by flame AAS on a Perkin-Elmer 3030 B spectrometer (USA) and a Thermo Electron Corporation Solar M6 photometer (USA). Each third sample was run in duplicate. The analytical accuracy was from 16 to 59% for gold and 5–59% for silver, at the p = 0.95 confidence depending on the Au and Ag contents (from 0.1 to 20 ppm Au and 0.2 to $2 \cdot 10^3$ ppm Ag, respectively).

3.2.3. Water chemistry

The ion composition of water samples was estimated by capillary electrophoresis (CE) on a Lumex Kapel 103P instrument (Russia). In CE methods, analytes migrating through electrolyte solutions under the influence of an electric field can be separated according to mobility of cations. The detection limits were from 10^{-3} to 10^{-4}% for different ions (Nature Protection Norms 14.2:4.167–2000), the RSD error did not exceed 15%.

Carbon was measured by IR spectroscopy on a Shumadzu Total Organic Carbon Analyzer, TOC-V_{CSH} (Japan). The method implies IR detection of CO_2 produced by HCl digestion of hydrocarbonates and carbonates. Total organic carbon (TOC) was determined by catalytical combustion of samples to CO_2, again measured by IR spectroscopy. The detection limit was 4 ppb and the analytical accuracy was better than 1.5%.

The contents of elements (Na, Mg, K, Ca, Al, Fe, Cu, Zn, Se, Ag, Au, Hg, Pb etc.) in the natural waters and mine drainage were determined by mass spectrometry with inductively coupled plasma (ICP-MS) on an Agilent Technologies Agilent 7500 quadrupole ICP-MS spectrometer (USA). The same method was applied to REE. The analytical accuracy was under 10% if the concentrations were an order of magnitude higher than the detection limit (see Table 1). The detection limits (see the Formula 1) were defined each time for each element as 3 × SD of the signal for the control water sample with the concentration of the analyte approaching 0, divided by the sensitivity coefficient (determined by analysis of standard element concentration), as recommended in the application manual of Agilent 7500. The sensitivity is determined by the number of counts per unit concentration.

Formula 1.

$$DL = (3\sigma \times \text{standard element concentration})/(S - B),$$

where DL is the detection limit; σ is the standard deviation (SD) from the control water sample signal; S is the standard element signal (concentration 10 μg/l); B is the control water sample signal at zero analyte concentration.

The composition of pore waters (Na, Mg, K, Ca, Al, Mn, Fe, Cu, Zn, Pb) was also determined by AAS (Thermo Electron Corporation Solar M6 spectrometer), with measured concentrations from 0.05 to $5 \cdot 10^5$ ppm. Total mercury in pore waters was analyzed by gold amalgamation with cold vapor AAS, on a 3030B Perkin-Elmer spectrometer (USA), with an MHS-20 mercury-hydrate detector. The detection limit was 0.02 ppb, and the analytical accuracy was 35%. The method was tested at the laboratory of the US National Bureau of Standards (Kovalev et al., 1998). Gold and silver were additionally determined on an Agilent Technologies Agilent 7500 quadrupole ICP-MS spectrometer (Table 1).

4. Results and discussion

4.1. Ursk tailings

The tailings at the Ursk site are dumped as two 10–12 m high piles of wastes from the primary ore and the gold-bearing weathering profile in

Table 1
Detection limits of elements for ICP-MS, ppb.

Element	Detection limit	Element	Detection limit
Na	4.2	Sb	0.0032
Mg	0.15	Te	0.008
Al	0.11	I	0.034
Si	18	Cs	0.0051
P	27	Ba	0.012
S	260	La	0.00093
Cl	9.5	Ce	0.0011
K	1.8	Pr	0.00013
Ca	0.41	Nd	0.00009
Ti	0.047	Sm	0.0005
V	0.0023	Eu	0.0001
Cr	0.052	Gd	0.0002
Mn	0.04	Tb	0.0001
Fe	1	Dy	0.0003
Cu	0.22	Ho	0.0001
Zn	0.57	Er	0.0001
As	0.0066	Tm	0.00009
Se	0.13	Yb	0.0002
Br	0.44	Lu	0.00007
Rb	0.0091	Au	0.0005
Sr	0.033	Hg	0.004
Ag	0.0021	Pb	0.021
Mo	0.0037	Th	0.0002
Cd	0.002	U	0.00031
Sn	0.0077		

the upper part of a natural ravine; nearby there are a flooded quarry and a gangue dump (Figs 3, 4a). Primary ore wastes (type I) are of gray color, rich in sulfide, and consist of barite, pyrite, quartz, and minor jarosite precipitates (Fig. 5). The percentages of pyrite, quartz, and barite inferred from major-element contents are, respectively, 35%, 20%, and 15%. Wastes of the weathered gold-bearing material (type II) are ginger-color and likewise contain barite, pyrite, and quartz (Fig. 5), but with smaller percentages of barite and pyrite (4% and 9%, respectively), larger contents of quartz (60%) and jarosite, with minor gypsum and goethite. Some of the minerals may be inherited from the primary ore compositions. Wastes II contain more abundant aluminosilicate minerals than wastes I (Fig. 5), notable amounts of muscovite, albite, and chlorite, and trace microcline.

Heavy mineral concentrate (HMC) samples contain 80% pyrite and 20% barite in wastes I and 64.5% pyrite, 35% barite, 0.5% galena and anglesite in wastes II. Diverse primary minerals are preserved in pyrite as inclusions and intergrowths, under 15 μm in size: galena, bornite (Fig. 6d), arsenopyrite (Fig. 6c), sphalerite (Fig. 6e), tennantite Cu_3AsS_3 (Fig. 6e), and chalcopyrite (Fig. 6f). Tennantite contains 3 wt.% Sb impurity and some chalcopyrites contain the impurities of 1 wt.% Ag and 0.5 wt.% Se. Other identified phases are altaite (PbTe; Fig. 6c,d), geffroyite $(Ag, Cu, Fe)_9(Se, S)_8$ (Fig. 6d), and mercury telluride with Ag impurity (Fig. 6f, g). Altaite and galena often bear up to 4 wt.% and 1.3 wt.% Se, respectively. Barite encloses naumannite (Ag_2Se; Fig. 6a) and mercury selenide with significant amounts of Ag and S: $Hg_{0.8}Ag_{0.2}Se_{0.7}S_{0.3}$ (Fig. 6a, b). Native gold was encountered only once in wastes I and never in wastes II, for the whole history of studies in the area. It was a submicron-scale particle in pyrite, with Cu and Ag impurities (Fig. 6h, i), of fineness 910‰ (28.6‰ Cu, 61.4‰ Ag). Most of gold in the Ursk tailings was inferred to be "invisible" (invisible gold refers to a very fine colloidal or cluster species, chemically or structurally bound with sulfides, and irresolvable by optical methods) (Cook and Chryssoulis, 1990; Kalinin et al., 2009; Kovalev et al., 2011; Zhmodik et al., 2012; Tauson et al., 2014), proceeding from the knowledge of disseminated gold in sulfides and from the lack of clastic Au. Gold is disseminated in wastes I and can be adsorbed on minerals (layered clay minerals such as kaolinite or montmorillonite, hydromica, Fe(III) compounds, etc.) in wastes II. Earlier fine dispersed gold was found in friable barite from the Ur ore field and identified analytically (Roslyakov et al., 1995).

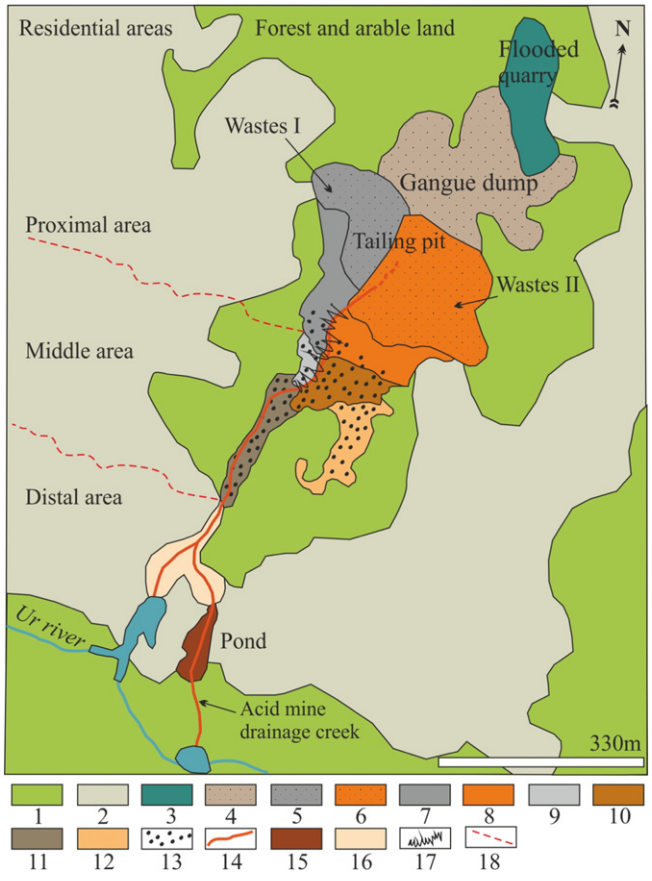

Fig. 3. Sketch map of Ursk tailings site located at 54°27′11.03″ N, 85°24′09.76″ E in Ursk Village. Legend: 1 = forests; 2 = residential areas; 3 = flooded quarry; 4 = gangue dump; 5, 6 = tailings: wastes I (5) and II (6); 7 = proximal zone of dispersion train composed of shed wastes I; 8 = proximal zone of dispersion train composed of shed wastes II; 9–12 = middle zone of train (shed wastes I and II); 13 = swampy part of contamination train; 14 = main AMD creek; 15 = pond; 16 = distal zone of train; 17 = road; 18 = intercalated wastes I and II; 19 = boundaries of train zones.

Wastes I have larger Fe, Cu, Zn, Se, Sr, Cd, Sn, Sb, Te, Ba, Hg and Pb, as well as S enrichments, while wastes II are richer in Na, Mg, Al, Si, K, Ca and Rb (Table 2). These patterns are due to mineralogy difference in the two types of wastes (Fig. 5). Residual Au and Ag are generally lower in wastes II (0.26 and 13 ppm) than in wastes I (0.5 ppm and 18 ppm), respectively (Table 2). Their contents in pyrite monofraction are quite low as well (0.5 ppm Au and 4.5 ppm Ag).

Sulfide-rich tailings deposited on the surface at the Ursk site are exposed to free oxygen supply (from air, rainfall, and floods) and the ensuing oxidation. The natural creek that drains the site has turned into an acid mine drainage stream (Fig. 4d) flowing into the Ur River (an Inya tributary). The AMD-affected swampy area downstream of the tailings became burnt out, partly void of vegetation, and covered by a thin mantle of shed material as far as the Ur River (Figs. 2,3), with remnant peat mounds rising above. Particles and dissolved elements, which migrate with drainage waters and re-precipitate, have produced a train around the tailings.

The material shed from the tailings undergoes hydraulic sorting, with coarser sand fractions settling near the discharge point and finer silt fractions carried away to longer distances (the classification of grain size fractions is according to Kachinsky (1958)), as it happens in tailings impoundments (Robertson, 1994). The related dispersion train of elements and particles can be divided conventionally into a proximal, middle and distal grain size zones located, respectively, at short (60 m), medium (130 m) and long (600 m) distances from the tailings (Fig. 3) (Gustaytis et al., 2010; Shcherbakova et al., 2010).

Dense layered segregations, or crusts and ochreous minerals precipitate from AMD waters in the proximal and intermediate zones. The crusts (mostly Fe(III) compounds) spatially coincide with ephemeral streams and exist also at the wastes/peat interface in the middle section. Most likely they were originally deposited on the surface and became buried under the material shed later from the waste piles.

As a result, the crusts bear significant amounts of barite, quartz, some pyrite, trace albite, and muscovite found in the tailings. Among new minerals, gypsum (in high percentages) and jarosite are clearly identifiable in X-ray patterns (Fig. 7). Poorly crystallized secondary iron compounds are hard to discriminate against the background primary minerals, but broad bases of peaks at 21.18 and 33.34 2Θ indicate possible presence of goethite (Fig. 7).

In the distal zone, the drainage waters form a pond (Figs. 3,4e), with its bottom sediments composed mainly of X-ray amorphous phases which may be a mixture of sulfates and Fe and Al hydroxides. Main minerals show broad and weak spectra (Fig. 7). The presence of schwertmannite and ferrihydrite can be inferred from comparison of the spectra with data by Bigham (1994) and with the Eh and pH values of the waters. Jarosite-group minerals exist to a large probability while the presence of goethite is less reliable. The sediments contain large percentages of layered clay minerals (illite, kaolinite, and montmorillonite; Fig. 7), either shed from the tailings or precipitated from waters. Note that layered clay minerals are also known from sulfide-bearing oxidized coal mine wastes (Jambor, 1994), and sulfide tailings (Valente and Gomes, 2009). The pond sediments may include diaspore (Fig. 7). The tailings primary minerals (barite, quartz, muscovite, microcline,

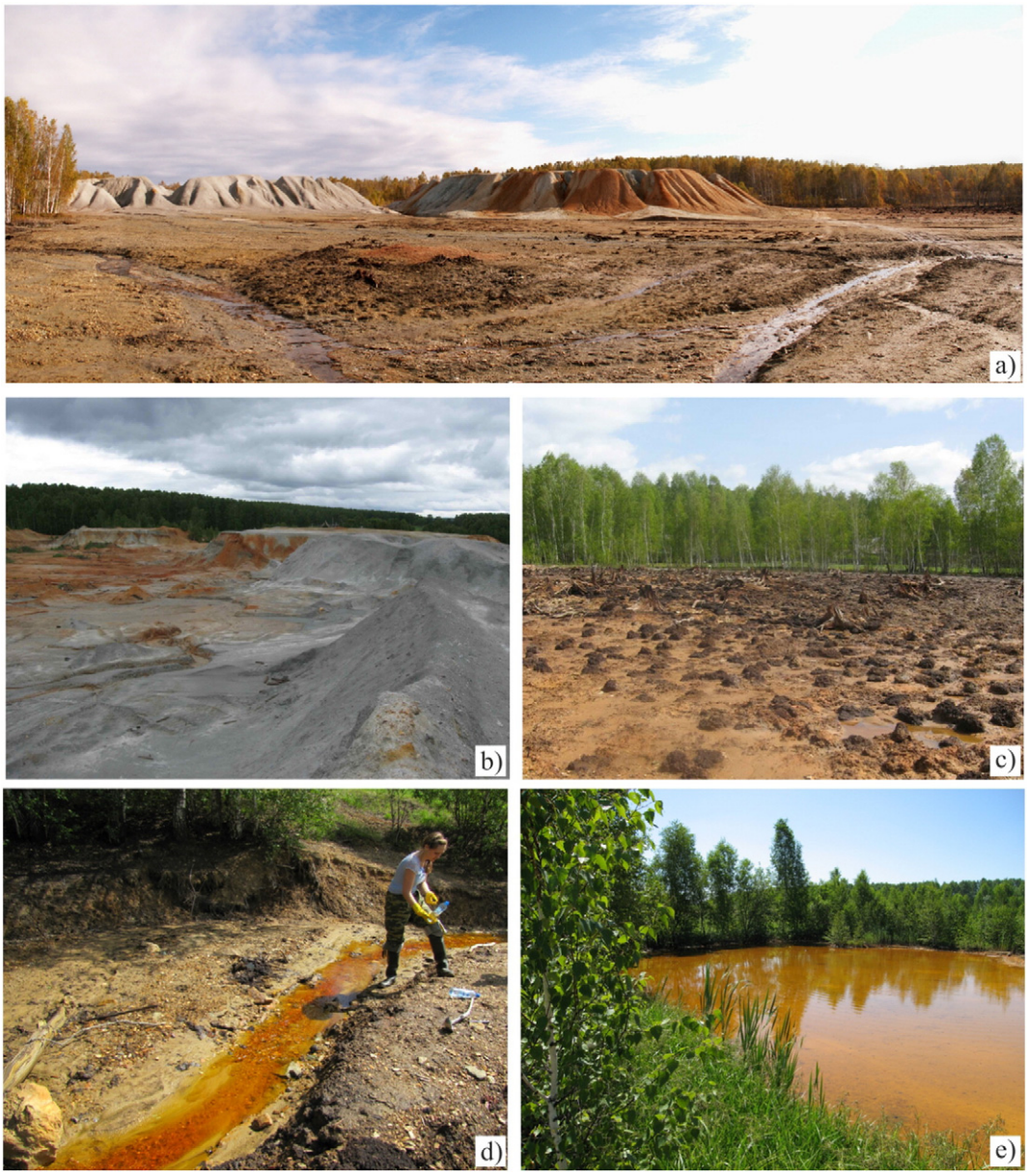

Fig. 4. Photographs of Ursk tailings site. a: piles of wastes I (left) and wastes II (right); b: gangue dump; c: swampy part of contamination train covered with wastes II; d: AMD streams in distal train zone; e: pond.

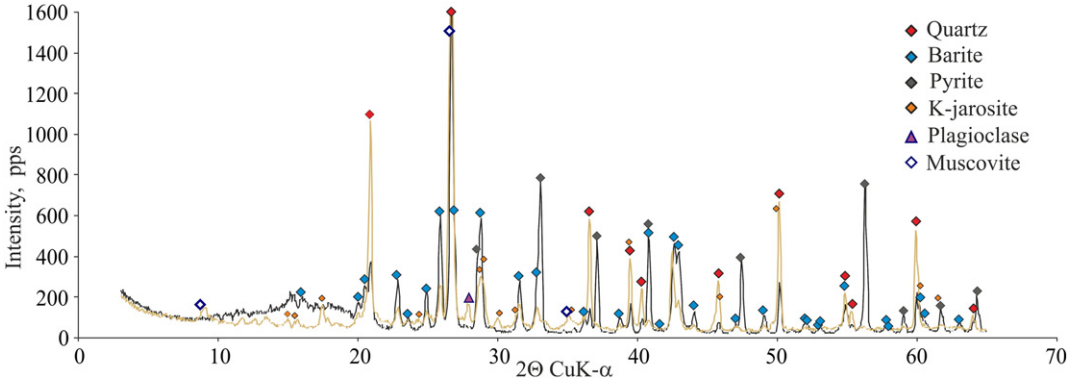

Fig. 5. XRD patterns of wastes I (black line) and II (beige line). Y axis shows intensity in pps (pulses per second); X axis shows CuK-α radiation.

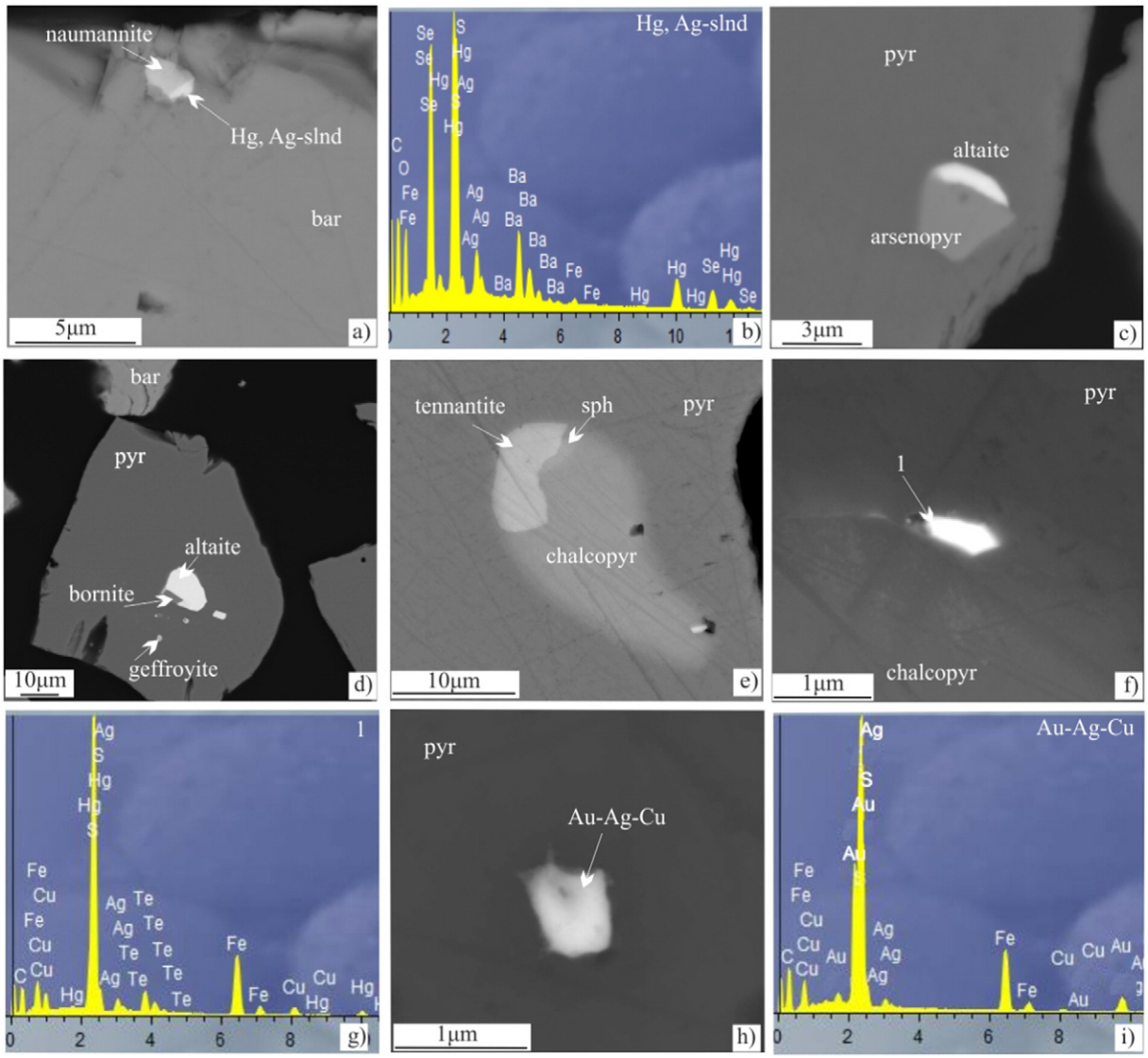

Fig. 6. SEM images of mineral inclusions in barite (bar) and pyrite (pyr). a: naumannite and Hg and Ag selenide (Hg, Ag-slnd) on the surface of barite; b: SEM–EDS from panel (a); c: altaite and arsenopyrite (arsenopyr) inclusions in pyrite; d: altaite, bornite, geffroyite inclusions in pyrite; e: pyrite intergrown with tennanite, sphalerite (sph), and chalcopyrite (chalcopyr); f: Hg and Ag telluride intergrown with chalcopyrite and pyrite; g: SEM–EDS from panel (f); h: elemental gold intergrown with pyrite; i: SEM–EDS from panel (h).

plagioclase, chlorite) brought by drainage and flood waters occur in minor amounts.

4.2. Chemistry of surface waters

Natural waters in the area of the Ursk tailings and AMD waters within the train (Table 3) have been classified according to major ions using the classifications by Perelman (1982) and Alekin (Reznikov et al., 1970). Natural waters upstream of the AMD discharge are cold (T ≤ 30 °C), oxygenated (13.5 ppm), with pH = 7.5, Eh = 515 mV, TDS ≤ 0.2 g/L, and have a hydrocarbonate chemistry with dominant Mg^{2+} and Ca^{2+}. The water chemistry we obtained is generally consistent with the data by B.A. Vorotnikov who studied waters in the area in the 1970s (Nesterenko et al., 1976). The waters show enrichments only in Si, As, Br, Sr, I, Ba and U (Table 3) being depleted in all other elements we analyzed.

The AMD waters are cold, with abundant Fe^{3+} that acts as a strong oxidizer, pH = 1.9, Eh = 655 mV, TDS ≤ 4.8 g/L, and have a sulfate composition with SO_4^{2-} reaching 3600 ppm, quite high enrichments of Al (>26 ppm) and Fe (780 ppm) and minor Cl (13 ppm). The abundances of Fe, Al, Cu, Zn and Pb are one or three orders of magnitude higher in AMD than in natural waters (Table 3) (Shcherbakova et al., 2010). The AMD waters are also more strongly enriched in As (630 ppb), Se (440 ppb), Te (28 ppb), Hg (11.4 ppb), and Cd (18 ppb) than the Ur River water, and have elevated contents of Si, P, Ti, V, Br, Rb, Sr, Mo, Sb, I, Cs, Ba, Th, and U (Table 3). The contents of Cr and Mn are slightly higher than in the Ur (Table 3).

AMD becomes less acid (pH increases from 1.9 to 2.5) away from the tailings, while Fe, Cu, Zn, Pb, Se, As, Cd, Te, Hg, Th and U decrease (Table 3). The concentrations of these elements are markedly lower in the pond distant from the tailings (points W-11, W-12, Table 3) than in the AMD creek in their immediate vicinity (point W-4, Table 3). This trend is due to sorption capacity of Fe(III), Al(III) and Si secondary minerals deposited on the bottom (Fig. 7) (Seal and Hammarstrom, 2003). There may be different interactions in the system "water–metals–organic matter–goethite": metals may either adsorb on goethite, or complex with organic ligands and then adsorb on goethite forming various mineral-organic clusters (Ali and Dzombak, 1996; Perelomov et al., 2011) or ternary complexes, for example goethite-Cu-FA) (Weng et al., 2008).

The AMD waters reacting with the Ur River at the inlet become neutralized and produce abundant particulate matter. The mixed waters

Table 2
Average values, ranges and standard deviations (SD) of element contents in tailings.

Element	Units	Wastes I	SD	Wastes II	SD	n
N	wt.%	<0.05	n.d.	<0.05	n.d.	3
C	wt.%	0.03/0.025–0.05	0.014	0.3/0.025–0.9	0.5	
H	wt.%	0.2/0.05–0.4	0.18	0.4/0.3–0.6	0.15	
S	wt.%	26/22–29	3.5	1.4/0.6–1.9	0.7	
Na_2O	%	<0.001	n.d.	0.36/0.001–0.6	0.2	6
MgO	%	<0.001	n.d.	0.1/0.001–0.3	0.13	
Al_2O_3	%	0.56/0.33–0.76	0.15	4.1/2–6	1.4	
SiO_2	%	16/6–23	5.9	58/26–70.3	17	
P_2O_5	%	<0.001	n.d.	<0.001	n.d.	
K_2O	%	0.09/0.04–0.17	0.04	0.53/0.2–0.9	0.21	
CaO	%	0.05/0.001–0.11	0.04	0.3/0.14–0.54	0.18	
TiO_2	%	0.14/0.1–0.18	0.03	0.3/0.18–0.46	0.09	
MnO	%	<0.001	n.d.	<0.001	n.d.	
Fe_2O_3	%	27/12.4–35	7.3	9.4/4.4–18.3	4.6	
LOI	%	19/7–24	6	5.4/2.5–8.6	2.52	
Cu	ppm	290/134–443	107	100/49.3–193	47.6	9
Zn	ppm	286/51–591	173	160/96–204	37	
Se	ppm	159/81–322	73	107/52–166	35	
Rb	ppm	17.8/12.2–24	5	34.8/19–54	10.2	
Sr	%	0.09/0.05–0.17	0.04	0.07/0.03–0.16	0.04	
Mo	ppm	6.3/2.8–11	2.6	5.6/2.2–7.9	2.1	
Cd	ppm	1.36/0.3–2.82	0.74	0.37/0.14–0.84	0.25	
Sn	ppm	13/6.5–25.6	6	5.5/0.98–11	3	
Sb	ppm	247/163–336	56	154.4/47.5–334	85.4	
Te	ppm	21.7/14.2–32	5.3	15/3.5–27	7	
Ba	%	23.7/11.4–40	10	13/3.2–39	10.3	
Hg	ppm	75/33–106	25.3	36/16–71	19	
As	ppm	B.D.L.	n.d.	0.03/0.01–0.06	0.02	
Pb	ppm	2867/1700–4100	929	2000/1100–2700	487	
Ag	ppm	18/11–25	4.9	13/8.2–21	5.4	
Au	ppm	0.5/0.21–0.71	0.19	0.26/0.13–0.49	0.15	

Note: n - is the number of samples; Wastes I are wastes of processed primary ore; Wastes II are weathered gold-bearing wastes; n.d. is no data; LOI is loss on ignition; B.D.L. is below detection limit.

(W-13, Table 3) are oxygenated, with pH = 7.1, Eh = 523 mV, TDS ≤ 0.2 g/L, and have an HCO_3^-–SO_4^{2-}–Mg^{2+}–Ca^{2+} composition. Away from the AMD inlet, the Ur water composition changes to HCO_3^-–Mg^{2+}–Ca^{2+}, oxygen increases, while TDS decreases (W-14–17, Table 3). The river water recovers its original ion composition 5 km downstream of the inlet (W-17, Table 3) (Shcherbakova et al., 2010). At the same distance, the contents of the analytes (Al, Mn, Rb, Sr, Cs, Ba, Cu, Zn, As, Se, Te, Pb, Fe) become commensurate with those upstream of the AMD discharge into the Ur (Table 3).

4.3. REE distribution

The Ur water not contaminated by AMD (pH = 7.5) has generally low REE abundances (Table 3) and is more depleted in LREE (till Nd) than in middle REE (Sm-Dy) and in HREE (Ho-Lu) relative to NASC (Taylor and McLennan, 1985) (Fig. 8, Table 3). The mobility of REE is pH dependent: REE form stable complexes with SO_4^{2-} in acid waters (pH < 5) but adsorb onto Fe and Al colloids and complex with CO_3^- at pH > 5, and become removed from the solution as pH increases further (Verplanck et al., 2004; Merten et al., 2005; Zhao-zhou et al., 2006; Lei et al., 2008; Sharifi et al., 2013; Vakh et al., 2013). Therefore, the pH = 1.9 AMD waters show much greater REE enrichments than the uncontaminated Ur water (Table 3), especially in La (190 ppb), Ce (470 ppb), and Nd (260 ppb). There is a weak positive Eu anomaly, most likely due to dissolution of aluminosilicates (plagioclase) in the tailings (Fig. 5). Middle REE are slightly higher than LREE and HREE (Fig. 8). These patterns with REE enrichments in general and high MREE in particular are typical of AMD waters (da Silva et al., 2009).

The REE concentrations decrease away from the tailings and become lower in the pond (pH = 2.9, point W-11, Fig. 8) than in the AMD waters (point W-4, Fig. 8). This may result from a slight pH increase and sorption on particulate matter (Figs. 4d–e, 7), as well as AMD enrichment with respect to Fe and Al which are in affinity with REE (LREE with Fe and HREE with Al) (Lei et al., 2008; da Silva et al., 2009).

The Ur waters affected by AMD (point W-13, Fig. 8) have higher REE abundances than the uncontaminated (point W-1, Fig. 8) river (Table 3). Note that unlike other REE patterns of natural waters and those contaminated by AMD (Fig. 8), curve W-14 is a broken line with two peaks, in Eu and Tm. However, they are rather due to the REE contents as low as the detection limits (Table 1), within the analytical accuracy 10%. In this respect, the curve is informative only as to the general trend of decreasing REE in contaminated waters. Particulate matter settles down away from the AMD discharge but REE depletion at 5 km is similar to that at the inlet; the normalized REE spectra become almost perfectly flat at this distance (point W-17, Fig. 8).

4.4. Gold and silver patterns

The waters of the Ursk tailings area contain dissolved (dissolved + colloidal) and particulate (suspended particles) gold and silver (Fig. 9). In uncontaminated natural waters, the particulate species is ten times more abundant than dissolved gold (0.007 ppb against 0.0006 ppb Au, Fig. 9a), which is similar to the tendency known also from other mining areas in Russia (Radomskaya et al., 2005). As for silver, its particulate and dissolved species are of the same order of magnitude: 0.008 ppb and 0.004 ppb, respectively (Fig. 9b).

The AMD waters bear high contents of gold, mainly in the dissolved form (Fig. 9a), ranging within 1.2 ppb in spring (May) and 0.4 ppb in summer (June) near the tailings. The Au contents in AMD are higher in spring when sulfide-bearing substances and acid waters are still frozen and the H_2SO_4 concentration is high (Ivanov and Bazarova, 1985; Takenaka et al., 1992). Freezing of the waters that contain some minor

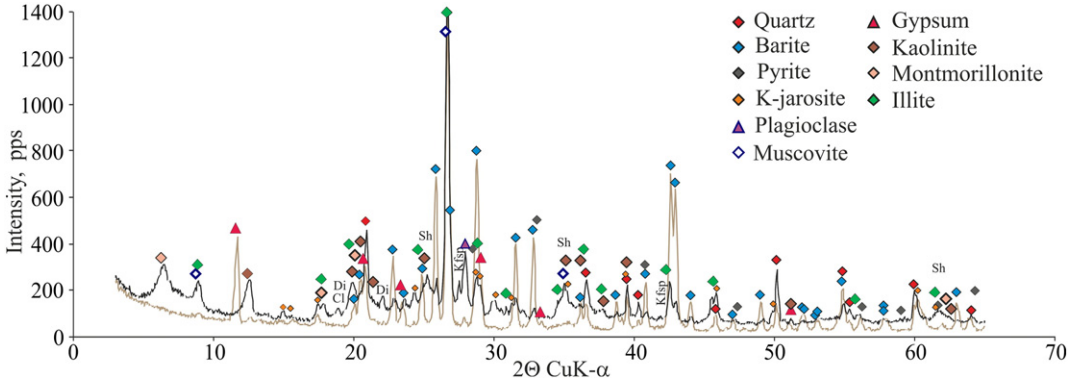

Fig. 7. XRD patterns of pond bottom sediments (black line) and layered crusts (beige line). Abbreviations stand for mineral names: Cl = chlorite, Di = diaspore, Kfsp = microcline, Sh = schvertmanite, ferrihydrite. Y axis shows intensity in pps (pulses per second); X axis shows CuK-α radiation.

Table 3
Water chemistry around Ursk tailings.

Elements	Units	W-1	W-3	W-4	W-11	W-12	W-13	W-14	W-15	W-16	W-17
pH		7.5	8.2	1.9	2.5	2.9	7.1	7.9	7.5	7.6	7.7
Eh	mV	515	530	655	660	698	523	530	465	471	485
O_2	ppm	13.5	8.2	< 0.2	< 0.2	< 0.2	8	12	7.5	8	12
TDS	g/L	0.2	0.22	4.8	2.6	1.5	0.2	0.36	0.35	0.28	0.32
TOC	ppm	13	6	14	10.5	9.5	7	6	6	5	5
Na^+	ppm	6.1	9.5	17	13	10	7.2	7	5.2	3.6	6.6
Mg^{2+}	ppm	9	7.5	100	62	43	11	5.2	8.6	5.2	8.3
K^+	ppm	1.5	6	0.9	0.7	1.5	1.5	1.4	1.4	0.7	1.5
Ca^{2+}	ppm	60	45	190	220	330	76	61	65	74	65
HCO^-_3	ppm	100.6	65.5	4.2	B.D.L.	7.5	19.3	263	232	174	201
SO^{2-}_4	ppm	15.6	63	3600	1917	1049	72	20	36	17	33
Cl^-	ppm	3.4	18	13	13	11	2.5	2.2	2.8	1.3	4.6
Al	ppm	1.2	0.9	>26	>26	>26	>26	1.4	1.25	0.94	0.92
Si	ppm	4.5	3.2	57	30	18	4.4	3.8	3.8	4	3.6
P	ppm	0.05	0.04	1	0.2	0.06	0.04	0.04	0.05	0.05	0.06
Ti	ppm	0.00086	0.0004	0.41	0.02	0.003	0.001	0.0008	0.0012	0.0005	0.003
V	ppm	0.001	0.00006	0.06	0.016	0.0003	0.0003	0.001	0.0008	0.00015	0.001
Cr	ppm	0.00024	0.0003	0.11	0.033	0.01	0.0002	0.0002	0.0002	0.0002	0.0005
Mn	ppm	0.25	0.13	17	15	11	0.8	0.2	0.3	0.04	0.25
Fe	ppm	0.2	0.14	780	280	24	0.29	0.1	0.2	0.24	0.5
Cu	ppm	0.0018	0.0012	2.5	0.97	0.3	0.006	0.0015	0.004	0.0012	0.0035
Zn	ppm	0.003	0.012	11	5.2	2.5	0.3	0.001	0.01	0.002	0.012
As	ppb	1.2	1.3	630	65	2.5	0.8	1.6	1.6	0.9	1.9
Se	ppb	0.6	1.2	440	52	13	1	0.59	0.83	1	0.8
Br	ppb	36	70	140	160	140	62	55	35	27	44
Rb	ppb	0.4	0.9	12	4.4	2.4	0.5	0.36	0.47	0.31	0.6
Sr	ppb	240	160	590	600	750	290	260	260	380	260
Mo	ppb	0.75	0.04	6.7	0.27	0.02	0.77	0.81	0.82	0.48	0.75
Ag	ppb	0.004	0.01	0.3	0.07	0.01	0.005	0.005	0.002	0.001	0.006
Cd	ppb	0.01	0.03	18	9	4.6	0.12	0.01	0.07	0.02	0.03
Sn	ppb	0.03	0.07	0.04	0.04	0.02	0.01	0.01	0.04	0.02	0.05
Sb	ppb	0.17	0.5	0.7	0.45	0.16	0.16	0.16	0.21	0.28	0.23

Element	Units	W-1	W-3	W-4	W-11	W-12	W-13	W-14	W-15	W-16	W-17
Te	ppb	0.01	0.02	28	3.5	0.25	0.01	0.01	0.01	0.01	0.01
I	ppb	7.4	21	25	19	16	14	12	8	7	12
Cs	ppb	0.02	0.01	0.2	0.05	0.03	0.02	0.003	0.06	0.04	0.035
Ba	ppb	50	130	10	23	18	44	47	52	39	69
La	ppb	0.06	0.01	190	110	63	0.2	0.023	0.11	0.01	0.32
Ce	ppb	0.13	0.02	470	260	150	0.44	0.04	0.23	0.01	0.7
Pr	ppb	0.02	0.002	61	31	17	0.045	0.005	0.025	0.004	0.08
Nd	ppb	0.063	0.006	260	130	68	0.17	0.02	0.1	0.006	0.32
Sm	ppb	0.015	0.003	61	30	15	0.04	0.005	0.02	0.003	0.08
Eu	ppb	0.006	0.006	17	8.2	4	0.013	0.003	0.01	0.005	0.002
Gd	ppb	0.02	0.003	55	31	18	0.06	0.007	0.03	0.005	0.1
Tb	ppb	0.003	0.0004	8	4.5	2.4	0.01	0.001	0.004	0.002	0.01
Dy	ppb	0.013	0.002	47	27	13	0.04	0.005	0.023	0.003	0.06
Ho	ppb	0.003	0.0004	9.3	5.3	2.6	0.01	0.001	0.006	0.002	0.012
Er	ppb	0.01	0.001	28	15	7.5	0.02	0.003	0.013	0.003	0.04
Tm	ppb	0.002	0.0002	4	2	1	0.003	0.001	0.003	0.002	0.005
Yb	ppb	0.01	0.001	25	13	6.5	0.02	0.004	0.013	0.003	0.03
Lu	ppb	0.002	0.0003	3.5	2	1	0.002	0.0005	0.002	0.002	0.006
Au	ppb	0.0006	0.002	1.2	0.01	0.001	0.001	0.001	0.001	0.001	0.001
Hg	ppb	0.027	0.61	11.4	0.38	n/d	0.18	n/d	0.31	0.23	0.036
Pb	ppb	0.1	0.5	110	59	49	0.23	0.06	0.3	0.13	0.7
Th	ppb	0.005	0.001	21	9	3	0.006	0.002	0.006	0.002	0.014
U	ppb	2.4	0.03	24	11	7	2	2.3	2.5	1.5	2.2

Note: May 2012; HCO^-_3 is calculated according to Inorganic Carbon data. B.D.L. is below detection limit. n/d is not determined. Samples represent waters upstream of AMD discharge (W-1), flooded quarry (W-3), AMD under the tailings (W-4), pond (W-11), pool formed by AMD flowing from pond, before discharge into the Ur River (W-12), AMD mixed with Ur water (W-13), Ur River, 200 m downstream of AMD discharge (W-14), Ur River 1 km downstream of AMD discharge (W-15), Ur River 3 km downstream of AMD discharge (W-16), Ur River 5 km downstream of AMD discharge (W-17).

amounts of N(III) coming to near-surface wastes from the atmosphere increases the concentration of HNO_2; the same mechanism may provide high HCl concentrations (Ptitsyn et al., 2006, 2007; Markovich, 2009). The strong acids maintain progressive oxidative dissolution of minerals, as well as dissolution of gold and its high contents in spring.

Dissolved + colloidal gold becomes lower while the particulate species increases (Fig. 9a) away from the tailings, where pH is slightly higher and suspended matter consisting of amorphous Fe(III), Al(III), and Si compounds is more abundant. This occurs on the pond bottom (Fig. 9a, point 11) covered with ochreous precipitates (Figs. 5e,7), where dissolved + colloidal and particulate gold species have commensurate percentages. However, particulate gold is much more abundant in a pool down the flow, which accommodates AMD from the pond (Fig. 9a, point 12): 0.01 ppb against 0.0014 ppb, respectively. Thus, particulate gold increases though remaining lower than the dissolved species.

Unlike gold, more silver in AMD occurs in the particulate form (to 1 ppb; Fig. 9b). The contents of dissolved + colloidal and particulate Ag are almost equal (0.1–0.3 ppb and 0.1–0.4 ppb, respectively; Fig. 9b) only in the immediate vicinity of the tailings and in the pond. In the mixed AMD-Ur River waters, both gold and silver are more

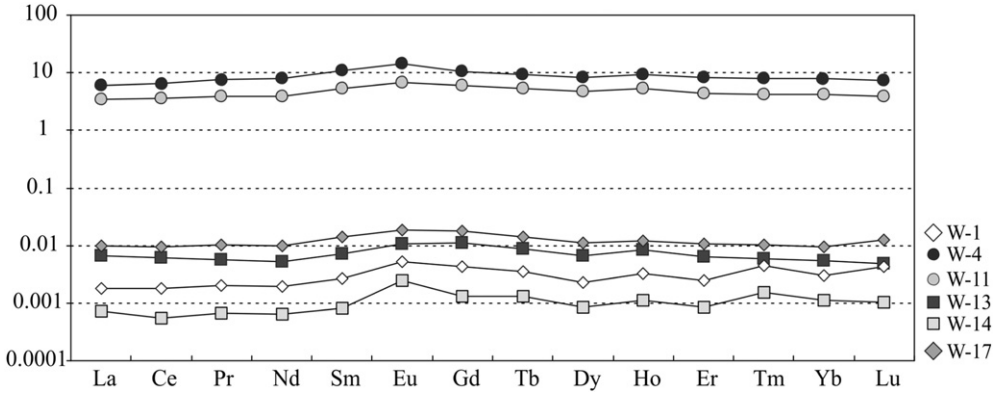

Fig. 8. NASC-normalized (Taylor and McLennan, 1985) REE patterns in waters around the tailings (in ppb). Samples (W) represent waters upstream of AMD discharge (W-1), AMD under wastes in proximal zone of contamination train (W-4), pond (W-11), AMD mixed with Ur River (W-13), Ur River, 200 m downstream of AMD discharge (W-14), and Ur River 5 km downstream of AMD discharge (W-17).

often particulate (Fig. 9), as suspension settled on the bottom can resuspend and travel long distances thereon.

Oxidation of sulfide materials produces sulfur-, chlorine-, OH-bearing, or mixed complexes (Mann, 1984; Stoffregen, 1986; Mironov et al., 1989; Vlassopoulos and Wood, 1990; Benedetti and Boulegue, 1991; Andrade et al., 1991; Colin and Vieillard, 1991; Dutova et al., 2006; Xia, 2008), which may be responsible for high contents of dissolved Au in the Ursk tailings area. According to the Pourbaix diagrams for the Au–S–Cl–H_2O and Au–S–H_2O systems (Vlassopoulos and Wood, 1990; Benedetti and Boulegue, 1991), the Au complexes more likely contain Cl and S. Furthermore, the Ursk tailings material being composed of cyanidation wastes, the cyanide complexes $Au(CN)_2^-$ may contribute to mine drainage (Leybourne et al., 2000).

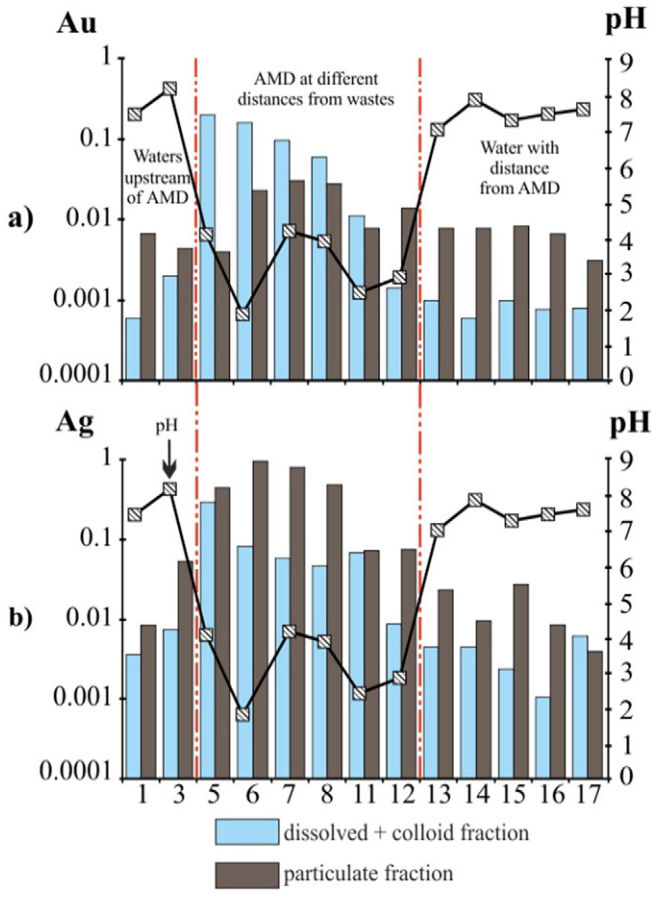

Fig. 9. Histograms (ppb contents) of dissolved and particulate gold (a) and silver (b) in waters of tailings area as a function of pH. May 2012. X axis shows sample numbers as in the map of Fig. 2: 1 = background uncontaminated waters upstream of AMD discharge; 3 = flooded quarry; 5 through 12 = AMD waters at different distances from the tailings; 13 = AMD mixed with Ur River; 14 = Ur River, 200 m downstream of AMD discharge; 15 through 17 = Ur River 1 to 5 km downstream of AMD discharge.

The transition from dissolved + colloidal to particulate gold species may result from destabilization of sulfur complexes at pH < 5 and sorption of uncomplexed gold on particles (see reactions 6 and 7) (Mironov et al., 1989; Benedetti and Boulegue, 1991; Xia, 2008). A similar case of sulfide tailings was reported from Canada (gossan tailings pile, Murray Brook massive sulfide deposit, New Brunswick) (Leybourne et al., 2000), where contents of dissolved gold decreased off the source from 19 ppb to 3 ppb, while Ag decreased to 2.9 ppb. The explanation was that degradation of cyanide along the flow path and within Gossan Creek allowed formation of colloidal gold (Leybourne et al., 2000). Proceeding from element migration patterns in water (see the Introduction section), we suggest that the changes in relative percentages of dissolved + colloidal and particulate gold and silver in the Ursk tailings area result from several processes: dissolution, ion exchange, adsorption, desorption, complexation, formation of colloids, reduction, and reactions with amorphous Fe(III) and organic compounds. Furthermore, silver as isomorphic impurity in alunite–jarosite group minerals (Mencheti and Sabelli, 1976; Rattray et al., 1996; Dill, 2001) enters colloids consisting mostly of Fe(III) compounds.

4.5. Pore water geochemistry

Pore water pressed out from the shed tailing material shares similar chemistry with AMD water (Tables 3 and 4). Its average pH and Eh values increase (from 1.5–1.8 to 3.5) and decrease (from 756–635 to 435 mV), respectively, away from the tailings. Pore water in surface bog peat, which interacts with the shed wastes, has pH = 2.2 and Eh = 534 mV while the respective values for peat buried at about 0.6 m below the surface are pH = 4.4 and Eh = 396 mV. The TDS contents are higher in pore water from the shed wastes than in AMD (Tables 3 and 4) and are close to the values in surface peat, but they decrease with depth from 4.4 to 1.4 g/L. C_{org} is the dominant component of pore water in buried peat (Table 4) but is lower in the bog peat which may lose more C_{org} being more strongly affected by AMD. TOC is also high in the pore water of shed wastes, possibly at the account of plant remnants.

Compared with AMD, the concentrations of Na, Mg, Al, K, Ca, Mn, Fe, Cu, Zn, Ag, Au, Hg and Pb in the pore water of wastes I are higher only for Na, K, Al, Fe, Cu, Ag, Hg and Pb (Table 4). The pore water of wastes II near the tailings and that of sand-silt waste material distant from the tailings contain all these elements in higher concentrations than AMD waters. This enrichment may be due to direct influence of wastes in the former

Table 4
Chemistry of pore water within the dispersion train.

Element	Units	Sand with plant remains: wastes I	Sand with plant remains: wastes II	Sand-silt wastes, with peat and ochreous precipitates	Bog peat	Buried peat
n		4	3	5	3	4
pH		1.8/1.1–2.2	1.5/1.2–1.7	3.5/1.45–4.8	2.2/2–2.3	4.4/3.5–6.4
Eh	mV	635/611–660	756/675–838	435/320–655	534/409–768	396/180–688
TDS	g/L	2.5/0.5–6	7.8/3–12	6.3/0.8–13	4.4/4–5	1.4/1–1.6
TOC	ppm	71/39–109	141/42–240	105/60–175	72/58–86	544/309–943
Na^+	ppm	20/15–23	65/15–115	25/13–39	29/13–42	15/11–18
Mg^{2+}	ppm	25/20–33	239/27–450	207/68–770	38/24.5–51	23/19–30
K^+	ppm	6.7/2.7–10	3.5/2.6–4.5	22/0.5–53	6/3.3–11	5.3/3–10
Ca^{2+}	ppm	86/10–130	475/180–770	383/52–520	393/102–757	226/117–371
SO_4^{2-}	ppm	1141/112–2922	3413/1317–5508	3343/320–8879	1790/1250–2338	307/208–404
Al	ppm	137/89–200	810/120–1500	448/42–2080	554/94–1389	108/58–223
Mn	ppm	4.5/1.3–7.2	18/10–27	34/12–130	19/2–40	9.1/1.1–16
Fe	ppm	987/29–2750	2590/1080–4100	1869/79–7500	894/117–1850	131/14.2–410
Cu	ppm	5.6/0.56–14	7.8/3.6–12	2.3/0.25–12	24/2–57	0.1/0.03–0.15
Zn	ppm	7/5.6–9.4	32/7–57	14.3/0.7–57	60/5–152	21/2–65
Ag	ppb	4.2/0.1–8.3	0.1/0.05–0.25	1.4/0.2–2.6	5.7/0.7–8.3	4.5/2.4–8.3
Au	ppb	0.2/0.15–0.25	0.1/0.15–0.2	0.2/0.1–0.25	2.1/1.25–5.5	1.8/0.5–5
Hg	ppb	102/6–163	122/100–145	454/88.5–1170	180/18–896	17/6–39
Pb	ppm	4/1.6–7	1.1/0.36–1.9	1.44/0.5–3.1	1.2/0.02–3.4	0.7/0.1–2.6

Note: The values are average contents in typical material of train, with ranges in denominator.
n - is the number of samples.

case and to low permeability of mud (Robertson, 1994) in the latter case. The element contents in bog peat are commensurate with or slightly above those in shed wastes but are lower than in buried peat at the 0.6 m depth (Table 4). Mercury in the pore water of shed wastes increases off the tailings from 102–122 ppb to 454 ppb in the most distal train part, and its contents in the peat pore water decrease with depth from 180 to 17 ppb.

Average contents of pore water gold and silver are higher in wastes I than in wastes II: 0.2 ppb Au and 4.2 ppb Ag (maximum 0.25 ppb Au and 8.3 ppb Ag against 0.1 ppb of both Au and Ag, maximum 0.2 ppb Au and 0.25 ppb Ag). The contents are quite high (0.2 and 1.4 ppb Au and Ag, respectively) in the sand-silt pore water in the distal train zone. Pore water gold is more abundant in peat (Table 4) than in wastes, most likely as a result of organic complexation (Vlassopoulos et al., 1990; Baranova et al., 1991; Bowell et al., 1993a,b; Varshal et al., 1996, 2000). Gold decreases with depth from 2.1 to 1.8 ppb. Silver is rather high in peat bog pore water (5.7 ppb) and likewise decreases depthward to 4.5 ppb.

4.6. Distribution of elements in bottom sediments

The Ur bottom sediments upstream of the AMD discharge have contents of rock-forming elements, e.g., Na, Mg, Al, Si, K, Ca and etc. (Table 5) higher than in both types of wastes (Table 2), but lower concentrations of Fe, Cu, Zn, and Pb (Table 5). Bottom sediments downstream of AMD consisting of shed cyanide wastes, which were sampled in the pond far from the tailings, show higher Mg, Al, K, Fe and Cu, Zn, Pb than the bottom sediments upstream of AMD (Table 5). The enrichment results from the spread and dissolution of wastes and subsequent precipitation of ochreous minerals (Figs. 4e,7) (Jambor, 1994; Bigham, 1994; Bigham et al., 1996; Equeenuddin et al., 2013) known to be good co-precipitators for elements (Seal and Hammarstrom, 2003; Hammarstrom et al., 2005; Dinu, 2010; Moiseenko et al., 2012; Carbone et al., 2013). Most elements are lower in bottom sediments 200 m far from the Ur-AMD confluence than in the pond but higher than in the Ur where they vary insignificantly away from the AMD discharge (Table 5). Namely, Cu, Zn, Pb remain slightly higher than in the non-contaminated Ur sediments upstream of AMD while Na, Mg, Al etc. are similar to the latter even 5 km downstream of it.

The contents of Au and Ag in the Ur bottom sediments are rather high (Table 5, Fig. 10) being inherited from gold deposits of the area (Nesterenko et al., 1976). Gold in the sampled river sediments (Table 5, point D-1) is three orders of magnitude higher than in soils of the Ur ore field (0.001–0.004 ppm) and far above the regional background (0.00045–0.0032 ppm) (Nesterenko et al., 1976). The shed wastes deposited on the AMD creek bottom store 0.5 ppm Au and 13 ppm Ag on average, exceeding the respective concentrations in uncontaminated natural bottom sediments in the area. The concentrations of gold and silver are markedly higher also in sediments of the pond than in the Ur sediments upstream of AMD (Fig. 10). The Au and Ag concentrations decrease down along the flow but remain higher than upstream of the AMD discharge (Fig. 10).

5. Conclusions

More than 80 years of mining at the Novo Ursk gold deposit have produced a natural-industrial system with changed patterns of

Table 5
Concentrations of elements in bottom sediments of streams around Ursk tailings.

Elements	Units	D-1	D-11	D-14	D-15	D-16	D-17
N	wt.%	0.05	0.12	0.05	0.05	0.2	0.2
C	wt.%	1.3	1.8	1.8	1.5	2.7	3.2
H	wt.%	0.6	1.1	0.6	0.6	0.8	0.8
S	wt.%	0	1	1	0	0	0
Na_2O	%	1.34	1	1.2	2.4	1.4	1.7
MgO	%	1.33	1.6	1.2	1.7	1.8	1.9
Al_2O_3	%	14	15	10.2	13	13.1	13.2
SiO_2	%	65	51	50	63	58.4	59.4
P_2O_5	%	0.13	0.16	0.15	0.17	0.19	0.2
SO_3	%	0.8	1.4	3.2	1.7	3.4	3.05
K_2O	%	1.7	2	1.6	1.4	2	1.9
CaO	%	1.1	0.5	0.9	3.4	3.6	3.6
TiO_2	%	0.84	0.8	0.6	0.8	0.8	0.8
MnO	%	0.1	0.05	0.04	0.2	0.22	0.3
Fe_2O_3	%	6.5	12.3	13.1	7	6.5	6.4
LOI	%	6.1	13	10.1	4.5	7.5	7.4
Cu	ppm	37	78	58	49	40	43
Zn	ppm	85	275	105	265	162	260
Ag	ppm	0.5	16	3.6	0.4	0.95	0.6
Cd	ppm	0.04	0.13	0.01	0.11	0.1	0.11
Ba	%	0.07	1.9	7	0.7	0.5	0.1
Au	ppm	0.14	0.66	0.25	0.03	0.2	0.3
Pb	ppm	18	1530	208	33	61	31

Note: June 2012; LOI = loss on ignition. Samples represent water upstream of AMD discharge (D-1), pond (D-11), Ur River, 200 m downstream of AMD discharge (D-14), Ur River 1 km downstream of AMD discharge (D-15), Ur River 3 km downstream of AMD discharge (D-16), Ur River 5 km downstream of AMD discharge (D-17).

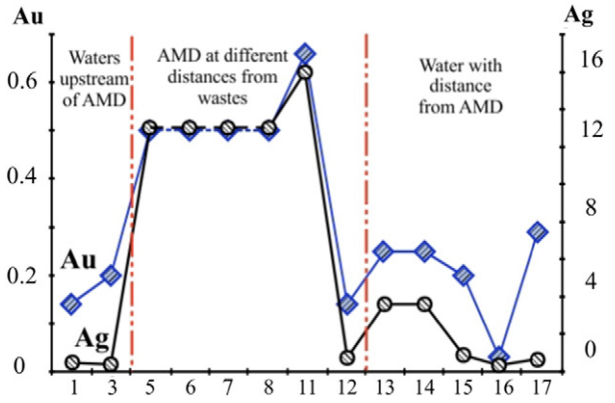

Fig. 10. Gold and silver (ppm contents) in bottom sediments. May 2011. X axis shows sample numbers as in the map of Fig. 2: Samples represent background uncontaminated waters upstream of AMD discharge (1), flooded quarry (3), AMD waters at different distances from the tailings (5 to 12), mixed AMD and Ur River waters (13), Ur River, 200 m downstream of AMD discharge (14), Ur River 1 to 5 km downstream of AMD discharge (15 to 17).

elements, including Ag and Ag. According to the reported analytical results, the redistribution patterns are as follows.

1. The Ursk tailings include processed primary ore (wastes I) and ore from the gold-bearing weathering profile (wastes II). Wastes I store residual noble metals: 0.5 ppm Au and 18 ppm Ag. Native gold in these wastes has been encountered only once over the whole history of research in the area. Gold occurs mostly as invisible species while silver either exists as impurity in preserved primary minerals (chalcopyrite, telluride and Hg selenide) or forms separate phases (geffroyite, naumannite). The concentrations of gold and silver in wastes II are lower (0.26 ppm Au and 13 ppm Ag) and gold particles never have been found. Gold in wastes of this type may adsorb on layered clay minerals (kaolinite, montmorillonite, etc.), hydromica, Fe(III) compounds, etc. Silver appears to be related mainly with alunite–jarosite group minerals.
2. Gold and silver become mobilized by oxidative dissolution of wastes and entrained with drainage waters. Gold migrates most often in the dissolved form along with colloids but particulate gold becomes more abundant away from the tailings, especially in the surface stream after mixing of the acid mine drainage and the alkalic Ur River waters. The gold concentration in AMD waters decreases away from the tailings as a result of deposition in bottom sediments. Silver likewise migrates with waters but, unlike gold, occurs in the particulate form in both natural waters and AMD.
3. Pore waters in the contamination train around the tailings have the highest contents of gold (up to 1.8–2.1 ppb) and silver (4.5–5.7 ppb) in peat, possibly because of organic complexing.

Acknowledgements

We wish to thank analysts L.V. Miroshnichenko, Zh.O. Badmaeva, L.N. Bukreeva, A.P. Zubareva, L.D. Ivanova, V.N. Ilyina, N.S. Karmanov, N.G. Karmanova, Yu.P. Kolmogorov, and O.L. Ogorodnikova for their work indispensable for this study.

We also appreciate thorough analysis and constructive criticism of the reviewers which helped us improve the manuscript.

The research was supported by grants 15-05-05362, 15-05-06950, 14-05-00668, 14-05-31280 from the Russian Foundation of Basic Research and was carried out as part of Integration Project 94 of the Siberian Branch of the Russian Academy of Sciences and the Ministry of Science and Education; also was carried out as part of Branch of the Earth Science the Russian Academy of Sciences — 5.1.

References

Al, T.A., Leybourne, M.I., Maprani, A.C., MacQuarrie, K.T., Dalziel, J.A., Fox, D., Yeats, P.A., 2006. Effects of acid-sulfate weathering and cyanide-containing gold tailings on the transport and fate of mercury and other metals in Gossan Creek: Murray Brook mine, New Brunswick, Canada. Appl. Geochem. 21 (11), 1969–1985.

Ali, M.A., Dzombak, D.A., 1996. Effects of simple organic acids on sorption of Cu^{2+} and Ca^{2+} on goethite. Geochim. Cosmochim. Acta 60 (2), 291–304.

All-Union State Standard # 31861–2012, 2013. Interstate Council for Standardization Metrology and Certification (ISC), Water: General Requirements for Sampling (ISO 5667-1:2006, NEQ; ISO 5667-2:1991, NEQ; ISO 5667-3:2003, NEQ). Standartinform, Moscow (60 pp. [in Russian]).

Alpers, C.N., Blowes, D.W., Nordstrom, D.K., Jambor, J.L., 1994. Secondary minerals and acid mine-water chemistry. Environmental geochemistry of sulfide mine-wastes. In: Jambor, J.L., Blowes, D.W. (Eds.), Waterloo, Ontario, Canada. Mineralogical Association of Canada, Short Course Series 22, pp. 247–270.

Andrade, W.O., Machesky, M.L., Rose, A.W., 1991. Gold distribution and mobility in the surficial environment, Carajas region, Brazil. J. Geochem. Explor. 40 (1–3), 95–114.

Auld, R.R., Myre, M., Mykytczuk, N.C.S., Leduc, L.G., Merritt, T.J.S., 2013. Characterization of the acid mine drainage microbial community using culturing and direct sequencing techniques. J. Microbiol. Methods 93 (2), 108–115.

Avramenko, V.A., Bratskaya, S.Y., Yakushevich, A.S., Voit, A.V., Ivannikov, S.I., Ivanov, V.V., 2012. Humic acids in brown coals from the southern Russian Far East: general characteristics and interactions with precious metals. Geochem. Int. 50 (5), 437–446.

Baker, W.E., 1978. The role of humic acid in the transport of gold. Geochim. Cosmochim. Acta 42 (6), 645–649.

Baranova, N.N., Varshal, G.M., Veliukhanova, T.K., 1991. Complexation of natural organic substances and their role in the genesis of gold deposits. Geokhimiya 12, 1799–1803 (in Russian).

Benedetti, M., Boulegue, J., 1991. Mechanism of gold transfer and deposition in a supergene environment. Geochim. Cosmochim. Acta 55 (6), 1539–1547.

Beneš, P., 1964. A radiotracer study of gold adsorption on glass from very dilute aqueous solutions. Radiochim. Acta 3 (3), 159–161.

Beneš, P., Smetana, J., 1966. A radiotracer study of gold adsorption on polyethylene from very dilute aqueous solutions. Radiochim. Acta 6 (4), 196–201.

Bessonenko V.V., Vinkim M.K. and Kuznetsov A.M. (1970). Geological map of the USSR. Scale 1:200,000, Series Kuzbass, Sheet N-45-XIV, Explanatory Note, Moscow. [in Russian].

Bigham, J.M., 1994. Mineralogy of ochre deposits formed by sulfide oxidation. Environmental geochemistry of sulfide mine-wastes. In: Jambor, J.L., Blowes, D.W. (Eds.), Waterloo, Ontario, Canada. Mineralogical Association of Canada, Short Course Series 22, pp. 103–132.

Bigham, J.M., Schwertmann, U., Pfab, G., 1996. Influence of pH on mineral speciation in a bioreactor simulating acid mine drainage. Appl. Geochem. 11 (6), 845–849.

Blowes, D.W., Ptacek, C.J., Jambor, J.L., 1994. Remediation and prevention of low-quality drainage from tailings impoundments. Environmental geochemistry of sulfide mine-wastes. In: Jambor, J.L., Blowes, D.W. (Eds.), Waterloo, Ontario, Canada. Mineralogical Association of Canada, Short Course Series 22, pp. 365–380.

Blowes, D.W., Ptacek, C.J., Jambor, J.L., Weisener, C.G., 2003. The geochemistry of acid mine drainage. Ref. Module Earth Syst. Environ. Sci. Treatise Geochem. 9, 149–204.

Bortnikova, S.B., Airiyants, A.A., Kolonin, G.R., Lazareva, E.V., 1996. Geochemistry and mineralogy of technogene deposits at the Salair mining and beneficiation works. Geochem. Int. 34 (2), 153–166.

Bortnikova, S.B., Gaskova, O.L., Airiyants, A.A., 2003. Impoundments: Origin, Evolution, and Environment Effects. Izd. SO RAN, Filial Geo, Novosibirsk (120 pp. [in Russian]).

Boulet, M.P., Larocque, A.C.L., 1998. A comparative mineralogical and geochemical study of sulfide mine tailings at two sites in New Mexico, USA. Environ. Geol. 33 (2–3), 130–142.

Bowell, R.J., 1992. Supergene gold mineralogy at Ashanti, Ghana: implications for the supergene behavior of gold. Mineral. Mag. 56, 545–560.

Bowell, R.J., Foster, R.P., Gize, A.P., 1993a. The mobility of gold in tropical rain forest soils. Econ. Geol. 88 (5), 999–1016.

Bowell, R.J., Gize, A.P., Foster, R.P., 1993b. The role of fulvic acid in the supergene migration of gold in tropical rain forest soils. Geochim. Cosmochim. Acta 57 (17), 4179–4190.

Carbone, C., Dinelli, E., Marescotti, P., Gasparotto, G., Lucchetti, G., 2013. The role of AMD secondary minerals in controlling environmental pollution: indications from bulk leaching tests. J. Geochem. Explor. 132, 188–200.

Cidu, R., Fanfani, L., Shand, P., Edmunds, W.M., Gijbels, R., 1994. Determination of gold at the ultratrace level in natural waters. Anal. Chim. Acta 296 (3), 295–304.

Cidu, R., Fanfani, L., Shand, P., Edmunds, W.M., Van'tdack, L., Gijbels, R., 1995. Gold mobility in waters from temperate regions. Proceedings of the 8th International Symposium on Water-Rock Interaction. 15–19 August, 1995. Water-Rock Interaction-8. Vladivostok, Russia, pp. 345–349.

Colin, F., Vieillard, P., 1991. Behavior of gold in the lateritic equatorial environment: weathering and surface dispersion of residual gold particles, at Dondo Mobi, Gabon. Appl. Geochem. 6 (3), 279–290.

Cook, N.J., Chryssoulis, S.L., 1990. Concentrations of invisible gold in the common sulfides. Can. Mineral. 28 (1), 1–16.

da Silva, E.F., Bobos, I., Matos, J.X., Patinha, C., Reis, A.P., Fonseca, E.C., 2009. Mineralogy and geochemistry of trace metals and REE in volcanic massive sulfide host rocks, stream sediments, stream waters and acid mine drainage from the lousal mine area (Iberian Pyrite Belt, Portugal). Appl. Geochem. 24 (3), 383–401.

Daryin, A.V., 2006. X-ray fluorescence analysis with synchrotron radiation (SR-XRF) for determination of elements in rocks. Methods. MVI- 3-2006. IGM SB RAS, Novosibirsk (in Russian).

de Haan, S.B., 1991. A review of the rate of pyrite oxidation in aqueous systems at low temperature. Earth Sci. Rev. 31 (1), 1–10.

de Oliveira, S.M.B., de Oliveira, N.M., 2000. The morphology of gold grains associated with oxidation of sulphide-bearing quartz veins at São Bartolomeu, central Brazil. J. S. Am. Earth Sci. 13 (3), 217–224.
Descostes, M., Vitorge, P., Beaucaire, C., 2004. Pyrite dissolution in acidic media. Geochim. Cosmochim. Acta 68 (22), 4559–4569.
Dill, H.G., 2001. The geology of aluminium phosphates and sulphates of the alunite group minerals: a review. Earth Sci. Rev. 53 (1–2), 35–93.
Dinu, M.I., 2010. Comparison of complexing ability of fulvic and humic acids in the aquatic environment with iron and zinc ions. Water Res. 37 (1), 65–69.
Dold, B., Fontbote, L., 2002. A mineralogical and geochemical study of element mobility in sulfide mine tailings of Fe oxide Cu–Au deposits from the Punta del Cobre belt, northern Chile. Chem. Geol. 189 (3–4), 135–163.
Dold, B., Wade, C., Fontbote, L., 2009. Water management for acid mine drainage control at the polymetallic Zn–Pb–(Ag–Bi–Cu) deposit Cerro de Pasco, Peru. J. Geochem. Explor. 100 (2–3), 133–141.
Druschel, G.K., Baker, B.J., Gihring, T.M., Banfield, J.F., 2004. Acid mine drainage biogeochemistry at Iron Mountain, California. Geochem. Trans. 5 (2), 13–32.
Dutova, E.M., Bukaty, M.B., Nevol'ko, A.I., Pokrovsky, D.S., Shvartsev, S.L., 2006. Hydrogenic concentration of gold in alluvial placers of the Egor'evsk area (Salair). Russ. Geol. Geophys. 47 (3), 364–376 (in Russian).
Equeenuddin, S.M., Tripathy, S., Sahoo, P.K., Panigrahi, M.K., 2010. Hydrogeochemical characteristics of acid mine drainage and water pollution at Makum Coalfield, India. J. Geochem. Explor. 105 (3), 75–82.
Equeenuddin, S.M., Tripathy, S., Sahoo, P.K., Panigrahi, M.K., 2013. Metal behavior in sediment associated with acid mine drainage stream: role of pH. J. Geochem. Explor. 124, 230–237.
Fairbrother, L., Brugger, J., Shapter, J., Laird, J.S., Southam, G., Reith, F., 2012. Supergene gold transformation: biogenic secondary and nano-particulate gold from arid Australia. Chem. Geol. 320-321, 17–31.
Falkner, K.K., Edmond, J.M., 1990. Gold in seawater. Earth Planet. Sci. Lett. 98 (2), 208–221.
Gibert, O., Rötting, T., Cortina, J.L., de Pablo, J., Ayora, C., Carrera, J., Bolzicco, J., 2011. In-situ remediation of acid mine drainage using a permeable reactive barrier in Aznalcóllar (Sw Spain). J. Hazard. Mater. 191 (1–5), 287–295.
Gitari, M.W., Petrik, L.F., Etchebers, O., Key, D.L., Iwuoha, E., Okujeni, C., 2008. Passive neutralization of acid mine drainage by fly ash and its derivatives: a column leaching study. Fuel 87 (8–9), 1637–1650.
Gleisner, M., Herbert, R.B., Kockum, P.C.F., 2006. Pyrite oxidation by Acidithiobacillus ferrooxidans at various concentrations of dissolved oxygen. Chem. Geol. 225 (1–2), 16–29.
Gustaytis, M.A., Lazareva, E.V., Bogush, A.A., Shuvaeva, O.V., Shcherbakova, I.N., Polyakova, E.V., Badmaeva, Z.O., Anoshin, G.N., 2010. Distribution of mercury and its species in the zone of sulphide tailing. Dokl. Earth Sci. 432 (2), 778–782.
Gustaytis, M.A., Lazareva, E.V., Myagkaya, I.N., Bogush, A.A., Shuvaeva, O.V., 2013. Mercury species in solid matter of dispersion of the Ursk tailing dispersion train (Ursk village, Kemerovo region, Russia). 22–27 September, 2012. Rome, Italy. The International Conference on Heavy Metals in the Environment (16th ICHMET) Abstracts. The E3S Web of Conferences journal. EDP Sciences 1, pp. 19007–19011.
Hamlin, S.N., 1989. Preservation of samples for dissolved mercury. Water Resour. Bull. Am. Water Resour. Assoc. 25 (2), 255–262.
Hammarstrom, J.M., Sibrell, P.L., Belkin, H.E., 2003. Characterization of limestone reacted with acid-mine drainage in a pulsed limestone bed treatment system at the Friendship Hill National Historical Site, Pennsylvania, USA. Appl. Geochem. 18 (11), 1705–1721.
Hammarstrom, J.M., Seal, R.R., Meier, A.L., Kornfeld, J.M., 2005. Secondary sulfate minerals associated with acid drainage in the eastern US: recycling of metals and acidity in surficial environments. Chem. Geol. 215 (1–4), 407–431.
Herrera, S.P., Uchiyama, H., Igarashi, T., Asakura, K., Ochi, Y., Iyatomi, N., Nagae, S., 2007. Treatment of acid mine drainage through a ferrite formation process in central Hokkaido, Japan: evaluation of dissolved silica and aluminium interference in ferrite formation. Miner. Eng. 20 (13), 1255–1260.
Heviánková, S., Bestová, I., Kyncl, M., 2014. The application of wood ash as a reagent in acid mine drainage treatment. Miner. Eng. 56, 109–111.
Hough, R.M., Noble, R.R.P., Reich, M., 2011. Natural gold nanoparticles. Ore Geol. Rev. 42 (1), 55–61.
Howe, K.J., Clark, M.M., 2002. Fouling of microfiltration and ultrafiltration membranes by natural waters. Environ. Sci. Technol. 36 (16), 3571–3576.
Ivanov, A.V., Bazarova, V.B., 1985. Chemical Weathering of Pyrite with Water and Various Solutions at Positive and Negative Temperatures, in: Migration of Elements in Permafrost. Nauka, Novosibirsk, pp. 115–124 [in Russian].
Jambor, J.L., 1994. Mineralogy of sulfide rich tailings and their oxidation products. Environmental Geochemistry of Sulfide Mine-Wastes. In: Jambor, J.L., Blowes, D.W. (Eds.), Waterloo, Ontario, Canada. Mineralogical Association of Canada, Short Course Series 22, pp. 59–102.
Jarvis, A.P., Rees, B., 2004. Mine water issues in the United Kingdom. In: Wolkersdorfer, C., Bowell, R. (Eds.), Contemporary Reviews of Mine Water Studies in Europe. Part 1. Mine Water and the Environment 23, pp. 162–182.
Jeen, S.W., Bain, J.G., Blowes, D.W., 2014. Evaluation of mixtures of peat, zero-valent iron and alkalinity amendments for treatment of acid rock drainage. Appl. Geochem. 43, 66–79.
Jung, M.C., 2001. Heavy metal contamination of soils and waters in and around the imcheon Au-Ag mine, Korea. Appl. Geochem. 16 (11–12), 1369–1375.
Kachinsky, N.A., 1958. Mechanic and microaggregate composition of soils. Methods. Izd. AN SSSR, Moscow (193 pp. [in Russian]).
Kalinin, Y.A., Kovalev, K.R., Naumov, E.A., Kirillov, M.V., 2009. Gold in the weathering crust at the Suzdal' deposit (Kazakhstan). Russ. Geol. Geophys. 50 (3), 174–187.
Korobushkina, E.D., Korobushkin, I.M., 1998. The role of microorganisms in the geochemistry of gold within the hypergenesis zone at the Darasun gold-sulfide deposit. Dokl. Earth Sci. 359A (3), 457–459.
Kovalev, S.I., Malikova, I.N., Anoshin, G.N., Badmaeva, Z.O., Stepin, A.S., 1998. Global and local constituents of the atmospheric precipitation of mercury in the Altai region. Dokl. Earth Sci. 363 (8), 1147–1149.
Kovalev, K.R., Kalinin, Y.A., Naumov, E.A., Kolesnikova, M.K., Korolyuk, V.N., 2011. Gold-bearing arsenopyrite in eastern Kazakhstan gold-sulfide deposits. Russ. Geol. Geophys. 52 (2), 178–192.
Lawrance, L.M., Griffin, B.J., 1994. Crystal features of supergene gold at Hannan South, Western Australia. Mineral. Deposita 29 (5), 391–398.
Lazareva, E.V., Tsimbalist, V.G., Shuvaeva, O.V., 2002. Arsenic speciation in the tailings impoundment of a gold recovery plant. Geochem. Explor. Environ. Anal. 2 (3), 263–268.
Lei, L.Q., Song, C.A., Xie, X.L., Li, Y.H., 2008. REE behavior and effect factors in AMD-type acidic groundwater at sulfide tailings pond, BS nickel mine, W.A. Trans. Nonferrous Metals Soc. China 18 (4), 955–961.
Leybourne, M.I., Goodfellow, W.D., Boyle, D.R., Hall, G.E.M., 2000. Form and distribution of gold mobilized into surface waters and sediments from a gossan tailings pile, Murray Brook massive sulphide deposit, New Brunswick, Canada. Appl. Geochem. 15 (5), 629–646.
Luptakova, A., Ubaldini, S., Macingova, E., Fornari, P., Giuliano, V., 2012. Application of physical–chemical and biological–chemical methods for heavy metals removal from acid mine drainage. Process Biochem. 47 (11), 1633–1639.
Lusilao-Makiese, J.G., Cukrowska, E.M., Tessier, E., Amouroux, D., Weiersbye, I., 2013. The impact of post gold mining on mercury pollution in the West Rand region, Gauteng, South Africa Original Research Article. J. Geochem. Explor. 134, 111–119.
Macías, F., Caraballo, M.A., Nieto, J.M., Rötting, T.S., Ayora, C., 2012. Natural pretreatment and passive remediation of highly polluted acid mine drainage. J. Environ. Manag. 104, 93–100.
Mann, A.W., 1984. Mobility of gold and silver in lateritic weathering profiles: some observations from Western Australia. Econ. Geol. 79 (1), 38–49.
Marescotti, P., Carbone, C., Comodi, P., Frondini, F., Lucchetti, G., 2012. Mineralogical and chemical evolution of ochreous precipitates from the libiola Fe-Cu-sulfide mine (Eastern Liguria, Italy). Appl. Geochem. 27 (3), 577–589.
Markovich, T.I., 2009. The special features of the kinetics of oxidation of divalent iron during sulfuric acid leaching of pyrrhotine with the participation of nitrous acid. Russ. J. Phys. Chem. 83 (1), 25–28.
McDonald, D.M., Webb, J.A., Musgrave, R.J., 2006. The effect of neutralization method and reagent on the rate of Cu and Zn release from acid rock drainage treatment sludges. Proceedings of the 7th ICARD. St. Louis, Missouri, USA, pp. 1198–1218.
Mencheti, S., Sabelli, C., 1976. Crystal chemistry of alunite series: crystal structure refinement of alunite and synthetic jarosite. Neues Jb. Mineral. Monat. 9, 406–417.
Merten, D., Geletneky, J., Bergmann, H., Haferburg, G., Kothe, E., Buchel, G., 2005. Rare earth element patterns: a tool for understanding processes in remediation of acid mine drainage. Chem. Erde Geochem. 65, 97–114.
Methods of Measurements M-MVI-80-2008, FR.1.31.2004.01278, 2008. AES and AAS Determination of Weight Percentages of Elements in Soil and Bottom Sediment Samples (St-Petersburg. [in Russian]).
Methods of Measurements MVI NSAM N 130-S, 2006. Flame AAS Determination of Silver in Rocks, Ores, and Processing Wastes (Moscow. [in Russian]).
Methods of Measurements MVI NSAM N 237-S, 2006. Extraction AAS Determination with Organic Sulfides in Mineral Deposits of Different Compositions (Moscow). ([in Russian]).
Mironov, A.G., Almukhamedov, A.I., Geletiy, V.F., Gliuk, D.S., Zhatnuev, N.S., Zhmodik, S.M., Konnikov, E.G., Medvedev, A.I., Plyusnin, A.M., 1989. Experimental Studies of Gold Geochemistry Using Radiotracers. Nauka, Novosibirsk (281 pp. [in Russian]).
Moiseenko, T.I., Dinu, M.I., Gashkina, N.A., Kremleva, T.A., 2012. Metal speciation in natural waters and metal complexing with humic matter. Dokl. Earth Sci. 442 (2), 267–271.
Moncur, M.C., Ptacek, C.J., Hayashi, M., Blowes, D.W., Birks, S.J., 2014. Seasonal cycling and mass-loading of dissolved metals and sulfate discharging from an abandoned mine site in northern Canada. Appl. Geochem. 41, 176–188.
Myagkaya, I.N., Lazareva, E.V., Gustaitis, M.A., Zayakina, S.B., Polyakova, E.V., Zhmodik, S.M., 2013. Gold in the sulfide waste-peat bog system as a behavior model in geological processes. Dokl. Earth Sci. 453 (1), 1132–1136.
Nesterenko, G.V., Roslyakov, N.A., Vorotnikov, B.A., Osintsev, S.R., Tsimbalist, V.G., 1976. Prospects of gold mineralization in the Northwestern Salair Ridge. Report, Contract 11–76, Laboratory 51 and Zapsibzoloto Company. Institute of Geology and Geophysics, Novosibirsk (51 pp. [in Russian]).
Nordstrom, D.K., 2000. Advances in the hydrogeochemistry and microbiology of acid minewaters. Int. Geol. Rev. 42 (6), 499–515.
Nordstrom, D.K., Alpers, C.N., 1999. Geochemistry of acid mine waters. The environmental geochemistry of mineral deposits. In: Plumlee, G.S., Logsdon, M.J. (Eds.), Part A: Process, Techniques and Health Issues. Reviews in Economic Geology 6, pp. 133–160.
Nyquis, J., Greger, M., 2009. A field study of constructed wetlands for preventing and treating acid mine drainage. Ecol. Eng. 35 (5), 630–642.
Ong, A.L., Swanson, V.E., 1969. Natural organic acids in the transportation, deposition and concentration of gold. Garterly Colo. Sch. Mine 64, 395–425.
Perelman, A.I., 1982. Chemistry of Natural Waters. Nauka, Moscow (154 pp. [in Russian]).
Perelomov, L.V., Pinskiy, D.L., Violante, A., 2011. Effect of organic acids on the adsorption of copper, lead, and zinc by goethite. Eurasian Soil Sci. 44 (1), 22–28.
Petrukhin, O.M., 1992. Analytical Chemistry. Chemical Methods of Analysis. Khimiya, Moscow (400 pp. [in Russian]).
Plumlee, G.S., 1999. The geology of mineral deposits. The environmental geochemistry of mineral deposits. In: Plumlee, G.S., Logsdon, M.J. (Eds.), Part A: Process, Techniques and Health Issues. Reviews in Economic Geology 6A, pp. 71–116.

Ptitsyn, A.B., Pavlyukova, V.A., Epova, E.S., Markovich, T.I., 2006. Cryogeochemical processes in the oxidation zone of sulfide deposits: experimental data. Dokl. Earth Sci. 411 (9), 1398–1400.
Ptitsyn, A.B., Pavlyukova, V.A., Epova, E.S., Markovich, T.I., 2007. Modeling cryogeochemical processes in the oxidation zone of sulfide deposits with the participation of oxygen-bearing nitrogen compounds. Geochem. Int. 45 (7), 726–731.
Radomskaya, V.I., Radomskii, S.M., Piskunov, Y.G., Kuimova, N.G., 2005. Biogeochemistry of noble metals in water streams of the Amur River Basin. Geoekologiya 4, 317–322 (in Russian).
Ran, Y., Fu, J., Rate, A.W., Gilkes, R.J., 2002. Adsorption of Au(I, III) complexes on Fe, Mn oxides and humic acid. Chem. Geol. 185 (1–2), 33–49.
Rattray, K.J., Taylor, M.R., Bevan, D.J.M., Pring, A., 1996. Compositional segregation and solid solution in the lead-dominant alunite-type minerals from Broken Hill, N.S.W. Mineral. Mag. 60 (402), 779–785.
Reith, F., McPhail, D.C., 2007. Mobility and microbially mediated mobilization of gold and arsenic in soils from two gold mines in semi-arid and tropical Australia. Geochim. Cosmochim. Acta 71 (5), 1183–1196.
Reith, F., McPhail, D.C., Christy, A.G., 2005. Bacillus cereus, gold and associated elements in soil and regolith samples from Tomakin Park Gold Mine in south-eastern New South Wales. J. Geochem. Explor. 85 (2), 81–89.
Reith, F., Stewart, L., Wakelin, S.A., 2012. Supergene gold transformation: secondary and nano-particulate gold from southern New Zealand. Chem. Geol. 320-321, 32–45.
Reznikov, A.A., Mulikova, E.V., Sokolov, I.Y., 1970. Analytical Methods for Natural Waters. Third edition. Nedra, Moscow (488 pp. [in Russian]).
Rieuwerts, J.S., Mighanetara, K., Braungardt, C.B., Rollinson, G.K., Pirrie, D., Azizi, F., 2014. Geochemistry and mineralogy of arsenic in mine wastes and stream sediments in a historic metal mining area in the UK. Sci. Total Environ. 472, 226–234.
Ríos, C.A., Williams, C.D., Roberts, C.L., 2008. Removal of heavy metals from acid mine drainage (AMD) using coal fly ash, natural clinker and synthetic zeolites. J. Hazard. Mater. 156 (1–3), 23–35.
Ritchie, A.I.M., 1994. Sulfide oxidation mechanisms: controls and rates of oxygen transport. Environmental Geochemistry of Sulfide Mine-Wastes. In: Jambor, J.L., Blowes, D.W. (Eds.), Waterloo, Ontario, Canada. Mineralogical Association of Canada, Short Course Series 22, pp. 201–246.
Robertson, D.E., 1968. The adsorption of trace elements in sea water on various container surfaces. Anal. Chim. Acta 42, 533–536.
Robertson, W.D., 1994. The physical hydrogeology of mine — tailings impoundments. Environmental Geochemistry of Sulfide Mine-Wastes. In: Jambor, J.L., Blowes, D.W. (Eds.), Waterloo, Ontario, Canada. Mineralogical Association of Canada, Short Course Series 22, pp. 2–17.
Roslyakov, N.A., 1981. Geochemistry of Gold in Supergene Environments. Nauka, Novosibirsk (238 pp. [in Russian]).
Roslyakov, N.A., Nesterenko, G.V., Kalinin, Y.A., Vasiliev, I.P., et al., 1995. Supergene Gold in the Salair Ridge Area. United Institute of Geology, Geophysics and Mineralogy, Novosibirsk (170 pp. [in Russian]).
Roychoudhury, A.N., Starke, M.F., 2006. Partitioning and mobility of trace metals in the Blesbokspruit: impact assessment of dewatering of mine waters in the East Rand, South Africa. Appl. Geochem. 21 (6), 1044–1063.
Samiullah, Y., 1985. Adsorption of platinum, gold and silver by filter paper and borosilicate glass and its relevance to biogeochemical studies. J. Geochem. Explor. 23 (2), 193–202.
Sarkar, D., Essington, M.E., Mirsa, K.C., 1999. Adsorption of mercury(II) by variable charge surface of quarz and gibbsite. Soil Sci. Soc. Am. J. 63 (6), 1626–1636.
Sarmiento, A.M., DelValls, A., Nieto, J.M., Salamanca, M.J., Caraballo, M.A., 2011. Toxicity and potential risk assessment of a river polluted by acid mine drainage in the Iberian Pyrite Belt (SW Spain). Sci. Total Environ. 409 (22), 4763–4771.
Seal, R.R., Hammarstrom, J.M., 2003. Geoenvironmental models of mineral deposits: examples from massive sulfide and gold deposits. Environmental Aspects of Mine Wastes. In: Jambor, J.L., Blowes, D.W., Ritchie, A.I.M. (Eds.), Mineralogical Association of Canada 31, pp. 11–50.
Sharifi, R., Moore, F., Keshavarzi, B., 2013. Geochemical behavior and speciation modeling of rare earth elements in acid drainages at Sarcheshmeh porphyry copper deposit, Kerman Province, IranOriginal Research Article. Chem. Erde Geochem. 73 (4), 509–517.
Shcherbakova, I.N., Gustaitis, M.A., Lazareva, E.V., Bogush, A.A., 2010. Migration of heavy metals (Cu, Pb, Zn, Fe, Cd) in the Ursk Tailing halo (Kemerovo Region). Chem. Sustain. Dev. 18 (5), 621–633 (in Russian).
Sima, M., Dold, D., Frei, L., Senilad, M., Balteanu, D., Zobriste, J., 2011. Sulfide oxidation and acid mine drainage formation within two active tailings impoundments in the Golden Quadrangle of the Apuseni Mountains, Romania. J. Hazard. Mater. 189 (3), 624–639.
Southam, G., Beveridge, T.J., 1994. The in vitro formation of placer gold by bacteria. Geochim. Cosmochim. Acta 58, 4527–4530.
Southam, G., Lengke, M.F., Fairbrother, L., Reith, F., 2009. The biogeochemistry of gold. Elements 5 (5), 303–307.
Stoffregen, R., 1986. Observations on the behavior of gold during supergene oxidation at Summitville, Colorado, U.S.A., and implications for electrum stability in the weathering environment. Appl. Geochem. 1 (5), 549–558.
Sun, J., Tang, C., Wu, P., Strosnider, W.H.J., Han, Z., 2013. Hydrogeochemical characteristics of streams with and without acid mine drainage impacts: a paired catchment study in karst geology, SW China. J. Hydrol. 504, 115–124.
Takenaka, N., Ueda, A., Maeda, Y., 1992. Acceleration of the rate of nitrite oxidation by freezing in aqueous solution. Nature 358 (27), 736–738.
Tauson, V.L., Kravtsova, R.G., Smagunov, N.V., Spiridonov, A.M., Grebenshchikova, V.I., Budyak, A.E., 2014. Structurally and superficially bound gold in pyrite from deposits of different genetic types. Russ. Geol. Geophys. 55 (2), 273–289.
Taylor, S.R., McLennan, S.M., 1985. The Continental Crust: Its Composition and Evolution. Blackwell Scientific Publications, Oxford-Boston (311 pp.).
Tokarev V.N., Shatilova G.A. and Kotik O.P. (2004). Geological Map of the Russian Federation. Scale 1:200000, Second edition. Series Kuzbass, Sheet N-45-XIV, Explanatory Note. St. Petersburg, 188 pp. [in Russian].
Tossell, J.A., 1996. The speciation of gold in aqueous solution: a theoretical study. Geochim. Cosmochim. Acta 60 (1), 17–29.
Tsimbalist, V.G., 1984. Determination of Gold and Silver in Geochemical Research: Methodological Guidelines. Publishing IgG SB AS USSR, Novosibirsk (53 pp. [in Russian]).
Vakh, E.A., Vakh, A.S., Kharitonova, N.A., 2013. The presence of REE in the waters of the supergene zone of sulfide ores, the Beresitovy deposit (Upper Priamurie). Russ. J. Pac. Geol. 32 (1), 105–115 (in Russian).
Valente, T.M., Gomes, C.L., 2009. Occurrence, properties and pollution potential of environmental minerals in acid mine drainage. Sci. Total Environ. 407 (3), 1135–1152.
Varshal, G.M., Velyukhanova, T.K., Korochantsev, A.V., Tobelko, K.I., Galuzinskaya, A.K., Akhmanova, M.V., 1996. The relation between the sorption capacity of the carbonaceous material in rocks for noble metals and its structure. Geochem. Int. 33 (7), 139–146.
Varshal, G.M., Veliukhanova, T.K., Chkhetiya, D.N., Kholin, Y.V., Shumskaya, T.V., Tyutyunnik, O.A., Koshcheeva, I.Y., Korochantsev, A.V., 2000. Sorption on humic acids as a basis of primary Au and PGE accumulation in black shale. Litol. Pol. Iskop. 6, 605–612 (in Russian).
Vasconcelos, P., Kyle, J.R., 1991. Supergene geochemistry and crystal morphology of gold in a semiarid weathering environment: application to gold exploration. J. Geochem. Explor. 40 (1–3), 115–132.
Verplanck, P.L., Nordstrom, D.K., Taylor, H.E., Kimball, B.A., 2004. Rare earth element partitioning between hydrous ferric oxides and acid mine water during iron oxidation. Appl. Geochem. 19 (8), 1339–1354.
Vlassopoulos, D., Wood, S.A., 1990. Gold speciation in natural waters: I. Solubility and hydrolysis reactions of gold in aqueous solution. Geochim. Cosmochim. Acta 54 (1), 3–12.
Vlassopoulos, D., Wood, S.A., Mucci, A., 1990. Gold speciation in natural waters: II. The importance of organic complexing experiments with some simple model ligands. Geochim. Cosmochim. Acta 54 (6), 1575–1586.
Wang, W., Wen, B., Zhang, S., Shan, X.Q., 2003. Distribution of heavy metals in water and soil solutions based on colloid-size fractionation. Int. J. Environ. Anal. Chem. 83 (5), 357–365.
Weng, L., Van Riemsdijk, W.H., Hiemstra, T., 2008. Cu^{2+} and Ca^{2+} adsorption to goethite in the presence of fulvic acids. Geochim. Cosmochim. Acta 72 (24), 5857–5870.
Wood, S.A., 1996. The role of humic substances in the transport and fixation of metals of economic interest (Au, Pt, Pd, U, V). Ore Geol. Rev. 11 (1–3), 1–31.
Xia, C., 2008. Associated Sulfide Minerals in Thiosulfate Leaching of Gold: Problems and Solutions (A Thesis Submitted to the Department of Mining Engineering in Conformity with the Requirements for the Degree of Doctor of Philosophy), Queen's University Kingston, Ontario, Canada (339 pp.).
Yudovich, Y.E., Ketris, M.P., 2004. Coal-hosted gold. In lithogenesis and geochemistry of sediments in the Tim-Ural Region. Trans. Inst. Geol. 116 (5), 80–109 (in Russian).
Zhao-zhou, Z., Liu, C., Wang, Z., Li, J., Zhou, Z.H., 2006. Inorganic speciation of rare earth elements in Chaohu Lake and Longganhu Lake, East China. J. Chin. Rare Earth Soc. 24 (1), 110–115 (in Chinese).
Zhmodik, S.M., Kalinin, Y.A., Roslyakov, N.A., Belyanin, D.K., Nemirovskaya, N.A., Nesterenko, G.V., Airiyants, E.V., Moroz, T.N., Bul'bak, T.A., Mironov, A.G., Mikhlin, Y.L., Spiridonov, A.M., 2012. Nanoparticles of noble metals in a supergene environment. Geol. Ore Depos. 54 (2), 141–154.